# Regional flood modelling for Horizons Flood Vulnerability Assessment (Task 3-1, FVA)

February 2026

horizons
REGIONAL COUNCIL

**Prepared for:**

Jon Roygard
Catchment Operations Group Manager

February 2026
Report No. 2026/EXT/1993
ISBN. 978-1-991351-97-5

**Prepared by:**

National Institute of Water & Atmospheric Research Ltd


| | | | | | |
|---|---|---|---|---|---|
| **CONTACT** | **24 hr Freephone 0508 800 800** | | **help@horizons.govt.nz** | | **www.horizons.govt.nz** |
| **SERVICE CENTRES** | **Kairanga**<br>Cnr Rongotea and Kairanga-Bunnythorpe Roads<br>Palmerston North<br><br>**Marton**<br>Hammond Street<br><br>**Taumarunui**<br>34 Maata Street | **REGIONAL HOUSES** | **Palmerston** North<br>11-15 Victoria Avenue<br><br>**Whanganui**<br>181 Guyton Street | **DEPOTS** | **Taihape**<br>Torere Road<br>Ohotu<br><br>**Woodville**<br>116 Vogel Street |
| **POSTAL ADDRESS** | Horizons Regional Council, Private Bag 11025, Manawatū Mail Centre, Palmerston North 4442 | | | | F 06 9522 929 |

# Regional flood modelling for Horizons Flood Vulnerability Assessment

***Prepared for Horizons Regional Council***

***June 2025***

Prepared by:
Alice Harang, Rose Pearson, Emily Lane, Shailesh Singh

For any information regarding this report please contact:

Alice Harang
Hydrodynamic Scientist
Environmental Hazards
+64 22 099 17 84
Alice.harang@niwa.co.nz

National Institute of Water & Atmospheric Research Ltd
PO Box 8602
Riccarton
Christchurch 8440

Phone +64 3 348 8987

NIWA CLIENT REPORT No: 2025133CH
Report date: June 2025
NIWA Project: WSP25502

| Revision | Description | Date |
|---|---|---|
| Version 1.0 | Final version sent to client for review | 22 May 2025 |
| Version 1.1 | Final version sent to client | 27 June 2025 |

| Quality Assurance Statement | | |
|---|---|---|
| | Reviewed by: | Gu Stecca |
| | Formatting checked by: | Rachel Wright |
| | Approved for release by: | Charles Pearson |

# Contents



## Tables

## Figures

# Executive summary

NIWA undertook a regional modelling study for Horizons Regional Council as part of a Flood Vulnerability Study in conjunction with WSP New Zealand Ltd. Twelve inundation domains cover the floodplains and river corridors in the Horizons Region. The upper catchments of the inundation domains are modelled using a hydrological model while the flood inundation in the inundation domains is modelled using a 2D hydrodynamic model. For each inundation domain, flood inundation due to 20-, 50-, 100-, 200-year rainfall design storms are modelled. Climate change scenarios for the 200-year rainfall design storm of +1˚C, +2˚C, +3˚C and +3˚C with Sea Level Rise were also modelled (the latter only for coastal flood inundation domains). For inundation domains with stopbanks, additional stopbanks-down scenarios (i.e., scenarios where the stopbanks have been removed) were modelled. Additional modelling of the 500- and 1000-year rainfall design storm for actual and climate change configurations were completed for the stopbank up scenario as an extension. This report outlines the methodology used in the regional modelling study and gives an overview of the results that were provided to Horizons Regional Council and used in the risk analysis.

# 1 Introduction

NIWA and WSP New Zealand Ltd are undertaking a joint study to contribute to the Horizons Regional Council's (Horizons) flood vulnerability assessment project. The study includes a region-wide assessment of the risks and vulnerabilities of the different towns in the region. As part of this study NIWA undertook a region-wide flood inundation assessment for the Horizons Region. Region-wide flood inundation hazard was modelled due to design rainstorms with Annual Exceedance Probabilities (AEP) of 5%, 2%, 1% and 0.5%, which correspond to Annual Return Intervals (ARIs, colloquially know as Return Periods) of 20-, 50-, 100- and 200-years. For the 0.5% AEP event, climate change scenarios corresponding to +1˚C, +2˚C and +3˚C over the current climate were also modelled (note that the recent epoch is already 1˚C above pre-industrial levels so these correspond to +2˚C, +3˚C and +4˚C above pre-industrial temperatures). For locations with stopbanks, additional stopbanks-down scenarios (i.e., scenarios where the stopbanks have been removed) were also modelled. These results were used in the risk assessment work and provided to Horizons.

This report outlines the methodology used in the modelling including the specifications of the flood domains where hydrodynamic modelling was undertaken, the creation of the Digital Elevation Models (DEMs), the design storms, the hydrological modelling in the upper catchments, the hydrodynamic modelling in the flood domains and the climate change methodology. Example results are given for the different Average Recurrence Intervals (ARIs), climate change warming increments, stopbanks up and down and sea level rise. The limitations of the regional-scale modelling are also discussed.

The results from this region-wide flood inundation assessment were used to calculate the vulnerability of the Horizons communities. The methodology for this flood vulnerability assessment is detailed in the Vulnerability Assessment Methodology - Appendix A of the Final Report, which outlines the approach used to assess community vulnerability. The Final Report further discusses the interpretation of these vulnerability results, placing them in the context of each communities' risk levels and the performance of flood protection schemes under various modelled scenarios. This comprehensive analysis helps explain the implications for community safety and the effectiveness of existing flood mitigation measures.

WSP's report on the Current State Analysis of Horizons Flood Vulnerability Assessment (Ashcroft et al. 2025) proposes a hydraulic model methodology framework which assesses modelling on a four-level scale from A to D (Level D being the highest). Table 1-1 presents the levels this modelling attains for each of the criteria presented in Table 4 of that report. While some of the criteria are level B/C, other criteria are only at level A giving it an overall level of A. The main reason behind this is because this is a regional model, it is not validated or calibrated to the same level that a local- or catchment-scale model would be. Not all flood structures are fully represented and there may be some artifacts in the DEM and roughness maps. These results should, however, give a good indication of the scope of the problem, where the highest levels of risk are likely to be and where further work (further LiDAR acquisition, higher level modelling etc.) is warranted to better characterise the flood hazard and vulnerability.

Additional modelling covering design rainstorms of 0.2% and 0.1% AEP (or 500- and 1000-year return periods) for current climate and climate change scenarios corresponding to +1˚C, +2˚C and +3˚C over the current climate for stopbank up scenarios only were undertaken as a variation on the contract. Details about these scenarios are presented in Appendix B.

**Table 1-1: Flood model level assessed against individual criteria.** Criteria taken from Table 4, WSP Client Report, Horizons Flood Vulnerability Assessment Current State Analysis (Ashcroft et al. 2025).

| Criteria | Level | Comment |
|---|---|---|
| **Data Methodology** | B/C | Report describes data and sources. Some data review, some limitations noted considering quality and sources of data. |
| **Asset Surveying** | B | Existing surveys of flood stopbanks were used but these weren't comprehensive. |
| **Channel Surveying** | B | Some cross-section data and river bathymetry estimation algorithms in addition to LiDAR used to characterise river channels. DEM hydraulically conditions to enforce downward flow. |
| **Hydrological Modelling** | B/C | Spatially and temporally varying design rainfalls used with TopNet hydrological model in upper catchments. |
| **Flood Events and Climate Change** | B/C | Design Rainfall AEPs from 0.1% to 5% modelled with lower AEP events also including Climate Change in terms of temperature increments. |
| **Terrain** | B | LiDAR-defined DEM prioritised over DSM where available. |
| **Land Cover** | B/C | Spatially varying roughness length defined from LiDAR data where available. A single roughness value is used where only the DSM was available. |
| **Cell Size/Resolution** | B/C | Adaptive grid with highest resolution of 8 m. |
| **Structures** | A/B | Flood stopbanks enforced (or removed) according to Horizons database, completed by the New Zealand Inventory of Stopbanks (NZIS). Other structures not included. No operational structures included. |
| **Stormwater Network** | A | No stormwater network included. |
| **Sensitivity Testing** | A/B | Not specifically undertaken in this study but basic sensitivity testing undertaken for locations outside Horizons Region. |
| **Validation and Calibration** | A | Limited comparison undertaken for Horizons locations. Overall national-scale methodology has been validated against events in case study locations (Waikanae, Tairāwhiti, Hawkes Bay). |
| **Outputs** | B/C | Maps of flood extents, depths, elevations, depth times velocity and rise rates for multiple AEP and Climate Change scenarios. |

# 2 Methodology

The methodology used for the Horizons Regional Council regional flood modelling follows that developed under the MBIE-funded Endeavour Programme Mā te Haumaru ō ngā puna wai ō Rākaihautū ka ora mō ake tonu[1]. This method consists of a cascade of models forced by design storms of different intensities, which allows for a consistent method at regional level and between gauged and ungauged catchments. The different steps of this method are presented in Figure 2-1 and will be described in the following sections. These different steps are integrated in a semi-automatic workflow managed by the open-source scheduler 'cylc' (Oliver et al. 2018).

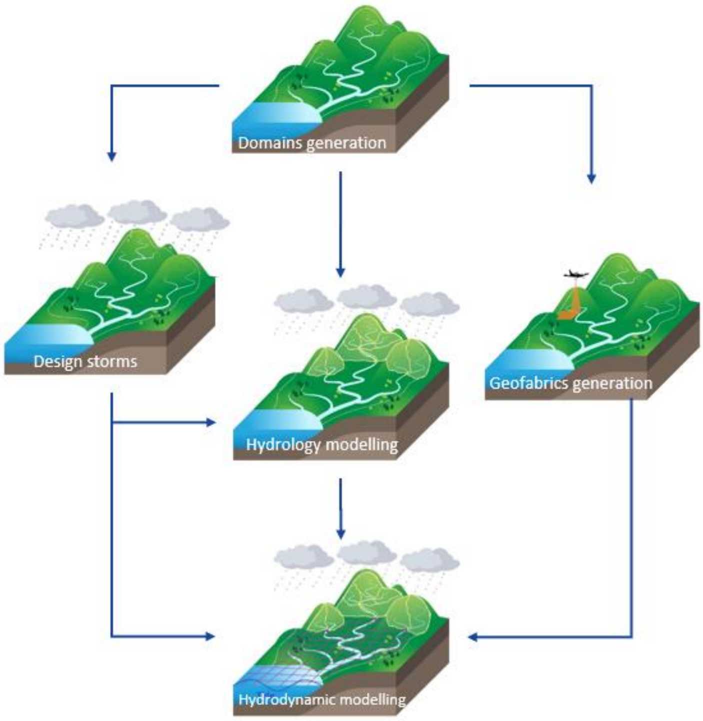


**Figure 2-1: Overall methodology from Mā te Haumaru ō te wai to generate floods maps from Design Storms.**

## 2.1 Flood modelling domains identification and specification

The first step of the workflow is the identification of flood modelling domains, carried out as a three-step procedure, resulting in the domains presented on Figure 2-2. Further information is given below but the basic steps are:

1. Specification of catchments based on identification of floodplains of interest,
2. Identification of flood inundation domain in catchment,
3. Identification of injection points where rivers flow into the flood inundation domain.

First, based on the topography and hydrology of the region, floodplains were roughly identified as the computational units where related or connected flood events can be observed. These domains were named after a major river or township in the domain. They consist of either a river floodplain (e.g., Ākitio Domain), different major rivers that share a floodplain (e.g., Turakina domain also containing the Whangaehu River), or a floodplain associated with a section of the river catchment

[1] http://niwa.co.nz/flood-resilience

(e.g., Upper Manawatū Domain associated with the Upper Manawatū Catchment, before the Manawatū Gorge, and lower Manawatū Domain associated with the lower part of the catchment). From these floodplains, we used a GIS-python tool in conjunction with the river network REC2.5[2], to identify the full catchment feeding this floodplain. The catchment is the hydrological domain associated with a given flood inundation domain where we ran the NIWA hydrological software for each scenario.

As a second step, including information from LINZ national databases, the flood inundation domains were identified along the river network from the mouth including catchment units having a maximum slope of less than 3% or minimum building and population density above a threshold. As this flood modelling requires high resolution ground elevation data and roughness data, the computational domains were also initially restricted to area where LiDAR data was available. As Horizons provided some DEMs (Digital Elevation Models) and a DSM (Digital Surface Model) covering the entire region, and after discussing the limitation of this type of data compared to LiDAR data, the restriction requiring LiDAR availability was relaxed. Following discussion with Horizons, we also included main transport infrastructure corridors in our modelling domains. Finally, a 500 m buffer was added to these domains for modelling purposes.

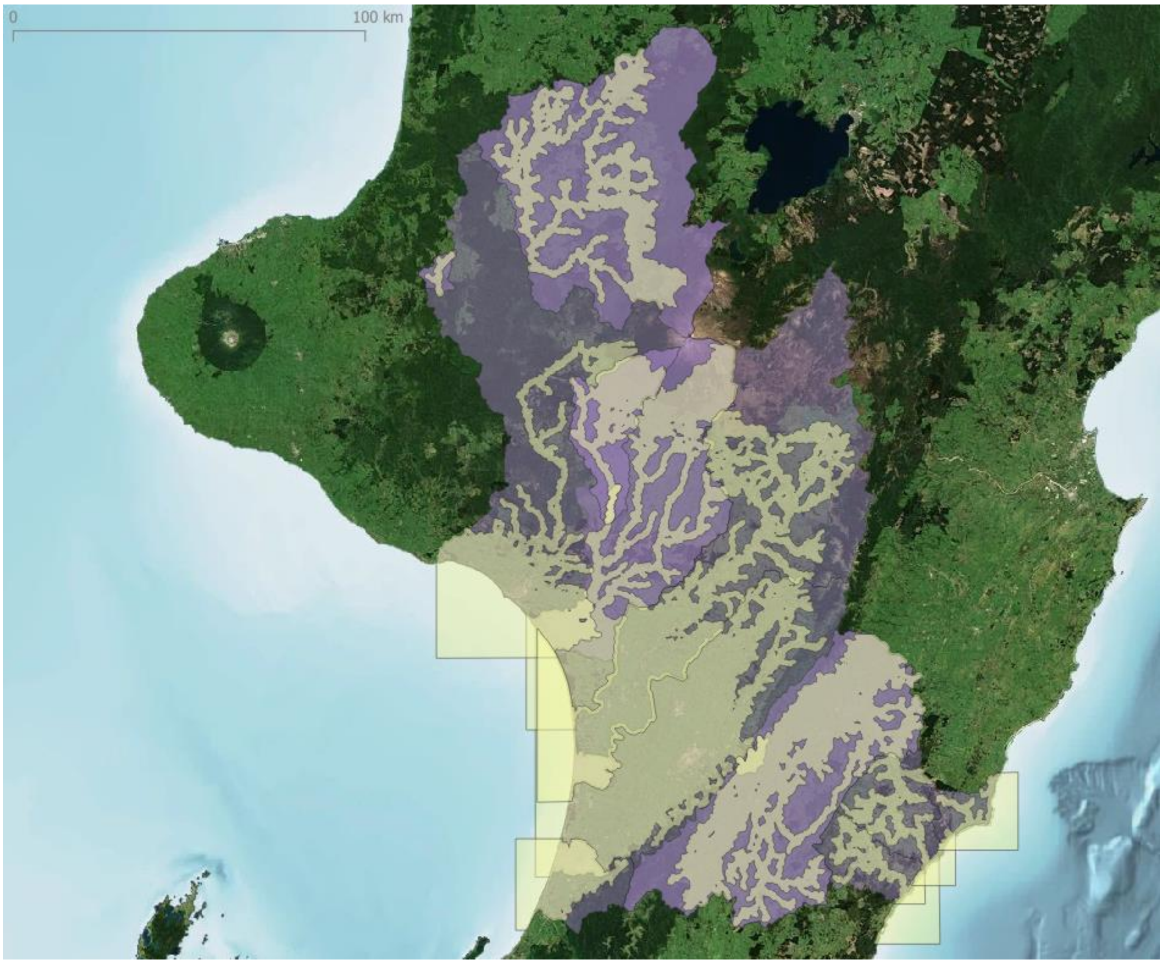


**Figure 2-2: Horizons regional modelling domains.** Domains where flood inundation modelling was undertaken (yellow), Catchments that feed these domains modelled by hydrological modelling (purple).

[2] https://niwa.co.nz/freshwater/river-environment-classification-2

As a last step, the injections points were identified as the intersections between the river network (at Strahler order 1, i.e., the complete network including the smallest river reaches) and the computational domain boundary. These injection points correspond to the location of the inlets where the flow hydrographs resulting from hydrological simulations are injected into the inundation model domains (see Figure 2-3).

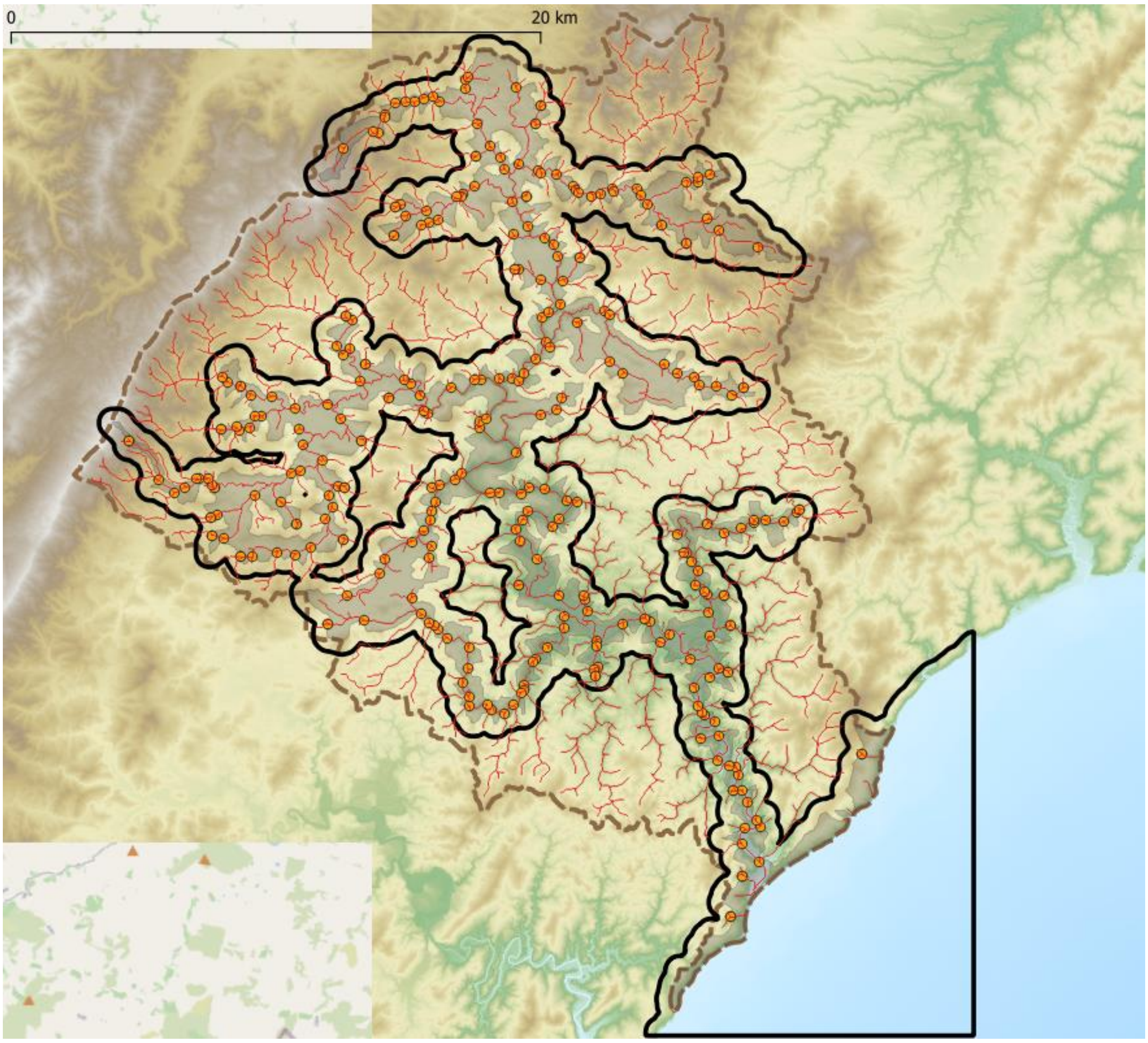


**Figure 2-3: Ākitio domain.** The domain for inundation modelling is within the boundary indicated by the black line and was generated as a buffer around the initially identified catchment units. The latter are the core of the domain and are indicated by greyed areas. Injection points (orange dots) are located at each intersection between a river or stream (red lines) from REC2.5 and the core of the domain. The extent of the full catchment or hydrological domain (for TopNet model) is indicated by the dashed brown line. The DEM (see later, in section 2.2) is visible in the background.

Table 2-1 lists the different inundation domains modelled through this study. The catchment area includes both the floodplain and the catchment area upstream of it. It is the area computed with the hydrological model. The computational area is the area of the inundation model for each domain (and it includes a sea corner for coastal domains). Finally, some catchments include or overlap with other computational domains. For example, the Whanganui catchment (as defined for this study), includes the Whanganui domain, but also the Whangamōmona, Taumarunui, Ohakune and most of the Turakina domain, as the Turakina River mouth is included in the domain as the Eastern boundary of the Whanganui floodplain. This overlap occurs because, on flood plains, flooding often spills beyond the bounds of one river into another. By overlapping the domains, we can capture flooding from multiple rivers. Without this, flooding that would naturally flow out onto the flood plain might build up against the edge of the computational domain, leading to it being artificially high. To avoid confusion, the results have been postprocessed so that for overlapping locations, the maximum inundation for a given AEP and temperature increment is given rather than the results for a single rainfall design storm event. Where the rectangular raster overlaps other domains the results from all flooded areas within the rectangle are given. The other information in this table are catchment properties, relating to scenarios explored for the different domains. Storm duration is the length of design storm chosen for each domain and is related to the size of the catchment and its time of concentration. The lower boundary of the catchment determines the model boundary condition; an outflow boundary condition is used for inland models and a tidal boundary (potentially including a different sea level rise on the east and the west coast) for the other models. For these coastal models, the tidal amplitude corresponding to Mean High Water Spring (MHWS) tide is also given. For all models with stopbanks, flood maps with stopbanks down are also produced (see Section 3.1 for more details). Finally, the overlapping computational models are listed in the last column.

**Table 2-1: List of inundation domain model locations.** Catchment properties are also given for each location.

| Computational domains | Storm duration (h) | Catchment area ($km^2$) | Computational area ($km^2$) (including sea corner) | Lower boundary (MHWS tidal amplitude in metres is given for coastal locations) | Stopbanks | Overlapping computational domains |
|---|---|---|---|---|---|---|
| Ākitio | 24 | 598 | 416 | East Coast (1.836) | no | Aohanga<br>Wainui-Herbertville |
| Manawatū | 60 | 6088 | 3079 | West Coast (2.236) | yes | Rangitīkei Upper Manawatū<br>Ōhau-Levin |
| Aohanga (Previously known as Owahanga) | 6 | 415 | 247 | East Coast (1.831) | no | Ākitio |
| Ohakune | 12 | 705 | 447 | Inland | no[3] | Turakina<br>Whanganui |
| Ōhau-Levin | 12 | 421 | 514 | West Coast (2.312) | yes | Manawatū |
| Rangitīkei | 42 | 4058 | 2533 | West Coast (2.451) | yes | Manawatū<br>Turakina |
| Taumarunui | 12 | 3813 | 1441 | Inland | yes | |
| Turakina | 60 | 3153 | 1903 | West Coast (2.591) | yes | Rangitīkei<br>Whanganui<br>Ohakune |
| Upper Manawatū | 60 | 3190 | 2357 | Inland | yes | Manawatū |
| Wainui-Herbertville | 6 | 195 | 340 | East Coast | no | Ākitio |

[3] Ohakune contains small flow retention structures but not identified as flood protection structures but detention embarkment (from Horizons Stopbanks database).

| Computational domains | Storm duration (h) | Catchment area (km²) | Computational area (km²) (including sea corner) | Lower boundary (MHWS tidal amplitude in metres is given for coastal locations) | Stopbanks | Overlapping computational domains |
|---|---|---|---|---|---|---|
| | | | | (1.817) | | |
| Whangamōmona | 6 | 76 | 40 | Inland | no | |
| Whanganui | 54 | 10525 | 1835 | West Coast (2.761) | yes | Turakina Ohakune |

## 2.2 DEMs

For each of the floodplains (inundation domains) identified for flood modelling, a two-dimensional digital elevation model (DEM) and a roughness map were created. Using a similar method to that for the national flood assessment project, hydrologically conditioned DEMs and roughness maps were generated for the entire region as a tile set of grids with a square mesh with a resolution of 8 m. These tiles were produced semi-automatically using the software tool GeoFabrics[4] (Pearson et al. 2023) and stored in a NetCDF file. This method provides a consistent and repeatable approach for combining multiple LiDAR, DEM datasets and ocean contours and applying hydrological conditioning. Figure 2-4 shows the process graphically.

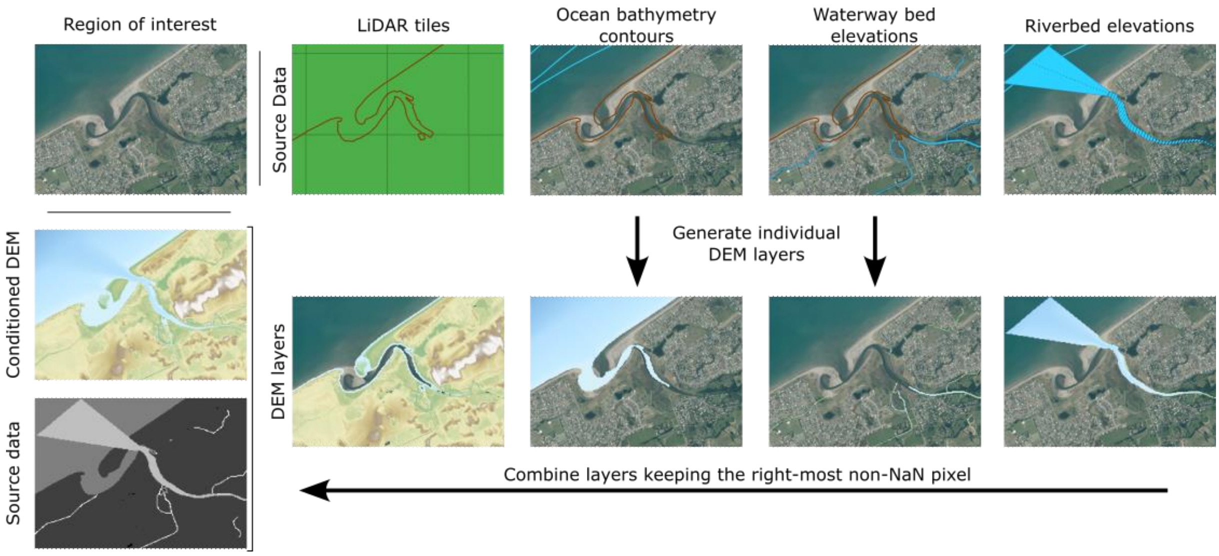


**Figure 2-4: Method for DEM and roughness generation by GeoFabrics.**

These tiles contain four variables: elevation above NZVD2016, roughness length (Zo), a data source classification, and a LiDAR source classification. At each floodplain the tiles needed to cover that domain were stitched together to generate the DEM and roughness map needed for flood modelling.

DEMs were generated using a combination of LiDAR data, which capture the above-ground surface elevation, and regional topographical datasets. In the case of rivers partially or totally submerged during the LiDAR survey, only the water surface elevation is recorded by the LiDAR, and the river

[4] https://github.com/rosepearson/GeoFabrics

bathymetry of the main riverbed is not captured. To deal with this problem, the Geofabrics framework applied hydraulic conditioning to the DEM, allowing the digging of rivers. Starting from the river mouth backward, the river-bed shape was derived from estimating the river cross-section necessary to allow the free discharge of a 2.33-year ARI event.

Specifically for this project, the method for generating these maps was adapted to the data available. For the elevation information, the priority was given to LiDAR data where it was available (as of December 2024), with a preference given to the more recent surveys (see Figure 2-5). Where no recent LiDAR was available in the Manawatū coastal area, the GtManawatu DEM, provided by Horizons and projected onto NZTM2000/NZVD2016 was used. Finally, where no recent LiDAR was available and outside of the region covered by the GtManawatu DEM, the digital surface model DSM provided by Horizons and projected onto NZTM2000/NZVD2016 was used.

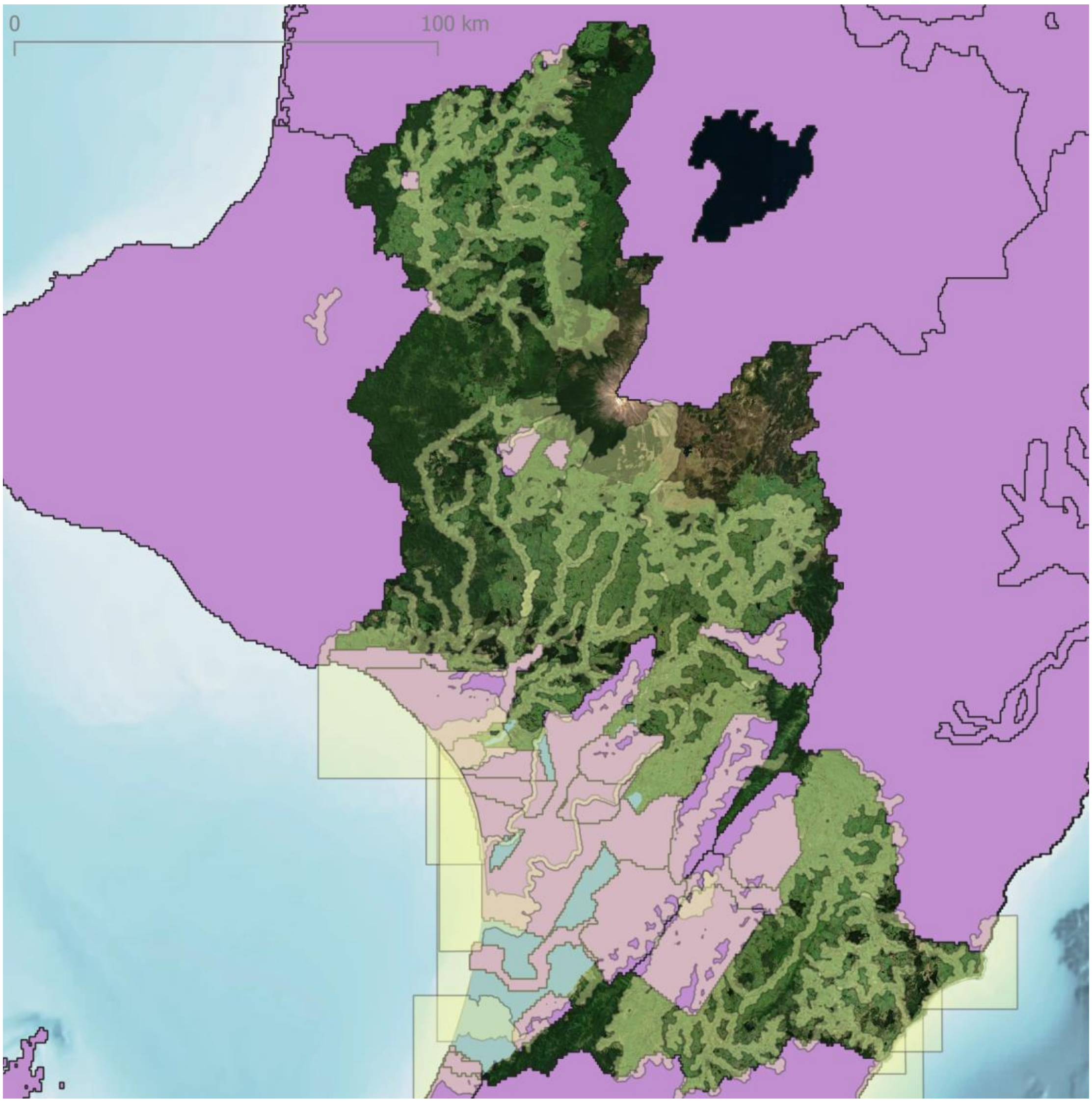


**Figure 2-5: Data used for DEM generation.** Purple: LiDAR available in 12/24, Blue: GtManawatu DEM, Background: DSM. Transparent yellow overlay: computational domains.

For hydrological conditioning, the OpenStreetMap (OSM) dataset was used to condition the waterways. The river mouths of the Whanganui, Whangaehu and Turakina were opened using an estimated mean annual flood flow. We also carried out complementary manual hydraulic conditioning of the lower part of the Ākitio, Manawatū, Aohanga, Ōhau-Levin, Rangitīkei, Turakina and Whanganui Rivers, placing the riverbed below the free surface at a depth determined using the cross-section data where available. Figure 2-6 presents an example of a DEM created using LiDAR data, DSM and hydrological conditioning.

The roughness coefficient was estimated from LiDAR where available using the mean elevation of the non-noise LiDAR returns above the ground and the standard deviation of the LiDAR point cloud. Where LiDAR was not available, a default Zo=0.004 value was used (see Figure 2-7).

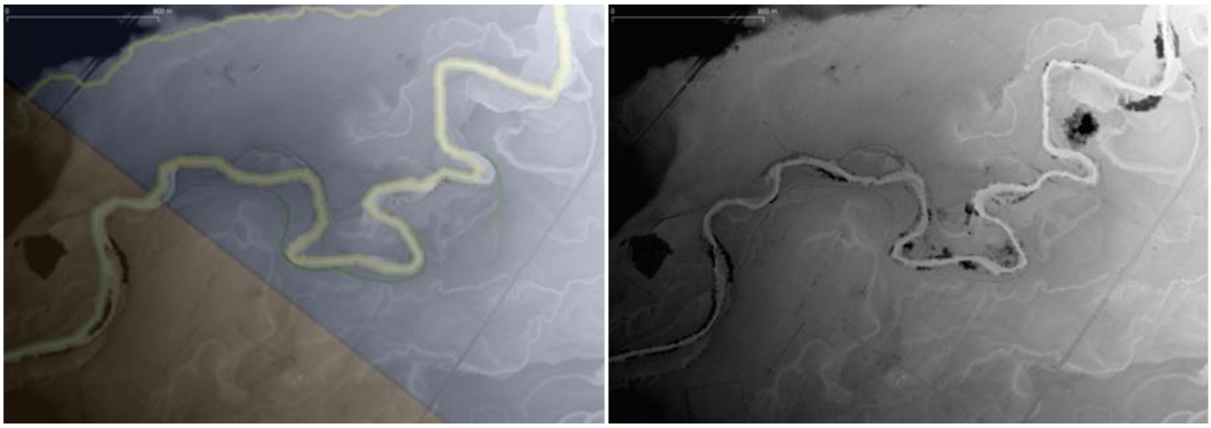

**Figure 2-6: Surface elevation along the Mangatainoka River, upstream of Mangamaire, at intersection of SH2 with Pukewahi road (Upper Manawatū Domain).** Left: DEM at 8 m resolution used for this study with blue: LiDAR data, orange: DSM data, yellow: river conditioning: green: stopbank enforcement. Right: DSM data at 1 m resolution: dark patch corresponds to vegetation and behave as flow obstacles. Colour bar ranges from 160 m (white) to 180 m (black).

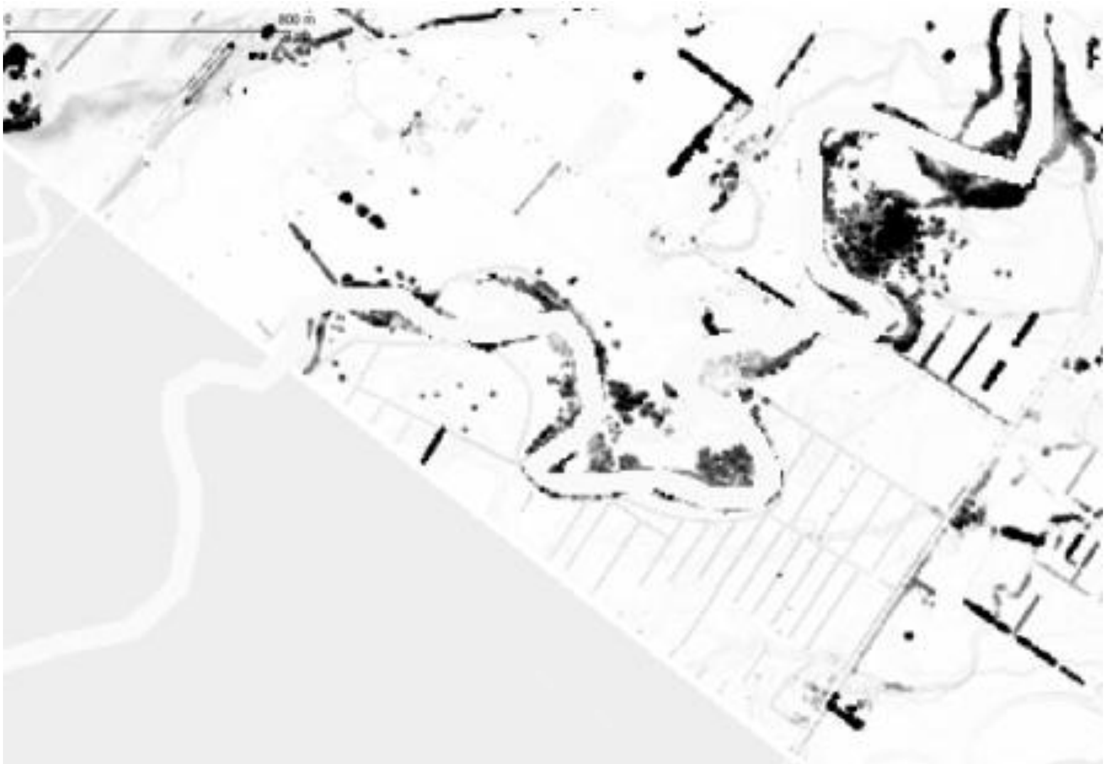

**Figure 2-7: Roughness length map in the Upper Manawatū Domain, on Mangatainoka River, upstream of Mangamaire, at intersection of SH2 with Pukewahi road.** Left bottom corner: default value where no LiDAR is

available; top right side: roughness extracted from LiDAR. Default value is implemented on rivers and water ways. Colour bar ranges from 1E-5 m (white) to 0.2 m (black).

Two sets of DEMs were created, one for the stopbank-up scenarios (where the stopbanks are included as they currently exist), and one for the stopbanks-down scenarios (where the stopbanks are removed to model residual risk) (see Figure 2-8). To identify the stopbanks, three datasets were combined and clipped to avoid overlaps: New Zealand Inventory of Stopbanks (NZIS), the Horizons stopbank dataset with no elevation (i.e., stopbank location only) and the Horizons Palmerston dataset with elevation (i.e., stopbank location and crest elevation). Precedence was given to the Horizons Palmerston dataset with elevation where it existed. The Horizons stopbank dataset with no elevation was given the second highest level of precedence. We included the features labelled Stopbank, Flood Walls, Detention Embankment, Flow Diversion Structure, Portable Flood Barrier, Guidebank, Property Mitigation Bund in the provided "RiverManagementAssetPolylineExport.shp" file. The NZIS dataset was included in areas where it included stop banks not otherwise represented in the other two datasets.
For the stopbanks-up DEMs, the stopbanks representation was enforced during the conditioning by locally modifying the DEMs at stopbank locations to correctly represent the crest heigh. Where crest heights were measured these were used directly; where no crest heights existed, the 1 m DEM of the area was generated blending the LiDAR data and the Horizons 1m DEM and used to identify the crest height.

For the stopbanks-down simulations, a separate set of DEM tiles were developed by removing the elevation data along each stopbank (as defined in the stopbank line files) and linearly interpolating to fill the gap. The combined stopbank line files were also used to control the generation of the computational grid for hydrodynamic modelling (see Section 2.5) These DEMs were created only for the domains where official stopbanks currently exist (see Table 2-1). The Ohakune Domain includes some small infrastructure but was not included in the list of domains that feature stopbanks as these were not considered flood protection but “detention embarkments” (in rural area) in Horizons Stopbanks database; only a stopbank up scenario was produced for this domain.


**Figure 2-8: DEM for the upper bank of the Whanganui River mouth.** Top panel: Aerial photo of the area with the location of the stopbanks highlighted as a red line; Middle panel: DEM with enforced stopbanks for the stopbanks-up configuration, Bottom panel: DEM with removed stopbanks for the stopbanks-down configuration.

## 2.3 Design Storms

Design storms were created for each catchment using NIWA's High Intensity Rainfall Design System - HIRDSv4[5] (Carey-Smith et al. 2018). This dataset gives gridded depth-duration-frequency (DDF) or intensity-duration-frequency (IDF) results across New Zealand for the current climate (based on observations).

For this study, an updated version of HIRDS was used based on research undertaken as part of the Mā te Haumaru ō te Wai Flood Resilience Endeavour programme. The main improvement is in the interpolation process that creates nationwide gridded estimates from gauge-specific extreme value parameters. Here, instead of elevation being used to guide the interpolation, as was done in HIRDSv4, the median annual maxima derived from NIWA's NZ Reanalysis project (NZRA) was used (Pirooz et al. 2023). NZRA is a full reanalysis weather model with a grid length of 1.5 km that is very close to completion. While still undergoing testing, the use of NZRA median annual maxima appears to provide more realistic estimates of rainfall depth than using topography alone, particularly in complex terrain.

To create the design storms, rainfall depths encompassing each catchment were extracted from HIRDS using the catchment boundary to delineate the size of the storm. To convert point rainfall depths (as provided by HIRDS) to areal depths, the catchment area was used to derive an areal

[5] See https://hirds.niwa.co.nz/

reduction factor. This reduction factor was applied to the total storm rainfall to account for the fact that rainfall extremes are calculated at point locations, but when larger areas are considered the storm intensity will be smaller than the point value for the same ARI. The total storm rainfall was then disaggregated to hourly resolution to emulate the typical temporal variation through the storm duration. Both the hyetographs used for temporal disaggregation and the areal reduction factors used follow the recommendations from Carey-Smith et al. (2018).

The effect of climate change on each design storm was included by incorporating two distinct changes. Firstly, the total rainfall volume was adjusted using temperature dependent multipliers derived from regional climate modelling performed over New Zealand. These factors, which are defined as the percentage increase in rainfall per degree of warming, vary as a function of both storm duration and storm return period – see Table 2-2, a reproduction of Table 6 in Carey-Smith et al. (2018). Secondly, the temporal shape of the storm was adjusted based on an analysis of how observed storm shapes change as a function of temperature. This research, which was done as part of the Mā te Haumaru ō te Wai Flood Resilience Endeavour programme, found that the most intense part of a rainstorm (in terms of time-period, relative to the total storm depth) becomes more intense with increasing temperature. In other words, the 'peakiness' of extreme rain events is expected to become peakier as the background temperature increases.

For each catchment, storms of multiple durations (6 hours through to 72 hours at six hourly increments) were modelled using the hydrological model (see details below) and the duration that gave the largest peak flow was used for inundation modelling (Duration values are presented in Table 2-1). For each flood domain, the same duration was used to define the 20-year, 50-year, 100-year and 200-year design rainstorm. Figure 2-9 shows an example 200-year design rainstorm of 54 hours duration for Whanganui.

**Table 2-2: Percentage change factors to project rainfall depths derived from the current climate to a future climate that is 1 degree warmer.** Reproduction of Table 6 in Carey-Smith et al. (2018).

| DURATION/ARI | 2 YR | 5 YR | 10 YR | 20 YR | 30 YR | 40 YR | 50 YR | 60 YR | 80 YR | 100 YR |
|---|---|---|---|---|---|---|---|---|---|---|
| 1 HOUR | 12.2 | 12.8 | 13.1 | 13.3 | 13.4 | 13.4 | 13.5 | 13.5 | 13.6 | 13.6 |
| 2 HOURS | 11.7 | 12.3 | 12.6 | 12.8 | 12.9 | 12.9 | 13.0 | 13.0 | 13.1 | 13.1 |
| 6 HOURS | 9.8 | 10.5 | 10.8 | 11.1 | 11.2 | 11.3 | 11.3 | 11.4 | 11.4 | 11.5 |
| 12 HOURS | 8.5 | 9.2 | 9.5 | 9.7 | 9.8 | 9.9 | 9.9 | 10.0 | 10.0 | 10.1 |
| 24 HOURS | 7.2 | 7.8 | 8.1 | 8.2 | 8.3 | 8.4 | 8.4 | 8.5 | 8.5 | 8.6 |
| 48 HOURS | 6.1 | 6.7 | 7.0 | 7.2 | 7.3 | 7.3 | 7.4 | 7.4 | 7.5 | 7.5 |
| 72 HOURS | 5.5 | 6.2 | 6.5 | 6.6 | 6.7 | 6.8 | 6.8 | 6.9 | 6.9 | 6.9 |
| 96 HOURS | 5.1 | 5.7 | 6.0 | 6.2 | 6.3 | 6.3 | 6.4 | 6.4 | 6.4 | 6.5 |
| 120 HOURS | 4.8 | 5.4 | 5.7 | 5.8 | 5.9 | 6.0 | 6.0 | 6.0 | 6.1 | 6.1 |

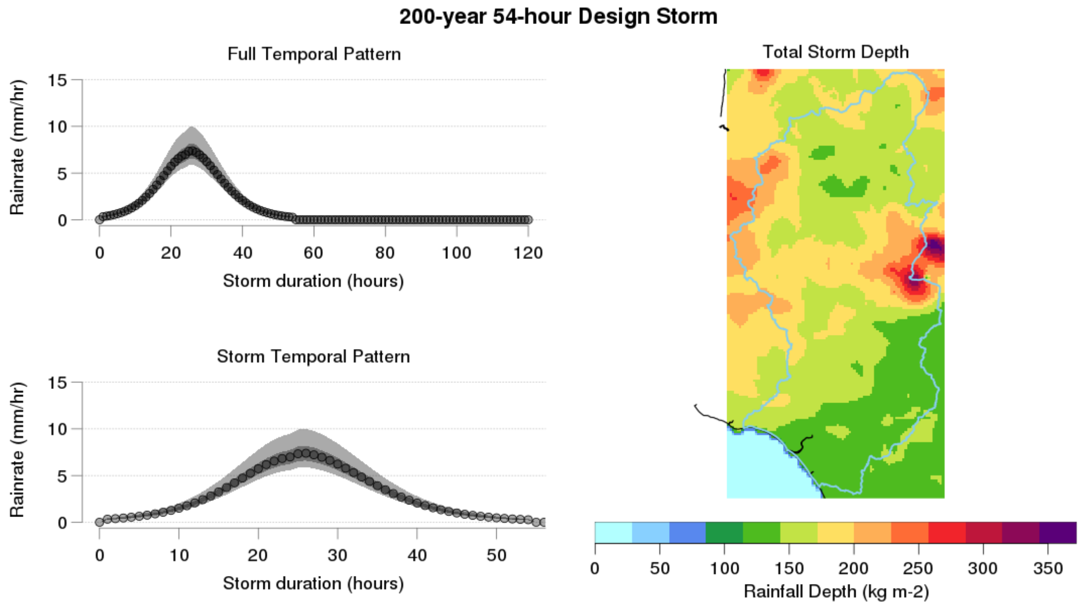


**Figure 2-9: Sample design storm for 200-year ARI and 54-hour duration event in the Whanganui catchment.** The left-hand-side shows the temporal rainfall pattern (grey shows the variation over the catchment) and the right-hand-side shows the spatial pattern of the total rainfall depth.

## 2.4 Hydrological modelling

The flood flows were modelled over the entire Manawatū-Whanganui region using the sub-catchment based hydrological model, TopNet (Clark et al. 2008; McMillan et al. 2016). The model combines a water balance model within each catchment with a kinematic wave routing algorithm through the river network (REC2.5). The Ki version of TopNet was used for this study, research suggests this version captures flood flows better than other uncalibrated model versions. Note that as TopNet is based on a network of sub-catchments (represented by the red lines in Figure 2-3), the results assume that all the water stays in the river channel and follows the path of the river network, so it does not capture out-of-banks flow or flow paths on floodplains that break the standard river network. Antecedent conditions at the start of the simulation were chosen as average flows. These flows were generated by forcing TopNet using 20 years of historical VCSN (Virtual Climate Station Network) data, a daily rainfall interpolation of observed data on a 0.1 degrees regular grid. The results from this were used to calculated percentile flow values at each outflow river reach (i.e., the reaches where the river flows into the sea). The 50$^{th}$ percentile flow for the main river reach for each domain was identified and the day that this occurred was used as the hot start for the hydrological simulation. This ensures that the entire catchment has physically realistic starting states. TopNet was then forced with the design storm rainfall, which produced hydrographs for each sub-catchment over the event. These hydrographs were outputted at the previously identified injection points (see Figure 2-3) and, together with tidal information and rainfall over the floodplain domains, were used to force the flood inundation models.

## 2.5 Hydrodynamic modelling

Hydrodynamic modelling was carried out using the BG-Flood software (Bosserelle et al. 2021). BG-Flood is an open-source 2D numerical solver of the Shallow Water Equations for modelling hydrodynamic systems. The source code, test cases and details regarding the evolution of the solver are available on the dedicated GitHub platform (https://github.com/CyprienBosserelle/BG_Flood). The solver can be applied to a variety of physical processes ranging from river hydrodynamics and floods modelling to storm surges and tsunami modelling.

The solver is optimised to work on GPU devices to exploit their inherent parallel computing capabilities and fast computing resources. BG-Flood uses an adaptative mesh generation method based on a block-uniform quadtree system, allowing cost-effective management of the computational time by locally adjusting the mesh size in prescribed locations to meet the level of refinement specified by the user. It is designed to run on UNIX based systems especially supercomputers such as New Zealand eScience Infrastructure (NeSI) but can also be used on Windows machines possessing a NVIDIA GPU.

To solve freshwater flood inundation, BG-Flood requires a DEM that represents the topography of the floodplain and a roughness map to represent land cover. For this work roughness was expressed in terms of the roughness length Zo to be used in a suitable logarithmic formulation of bottom friction (Smart et al. 2004). This is an alternative to the more commonly used Manning equation. We prefer the above logarithmic law as it more accurately captures the dependence of the friction slope on the water depth across the entire range of flow depths.

The model is built within the boundaries of the inundation domain and applies a spatially and temporally varying rainfall design storm discussed in Section 2.3. It is also forced by a time-varying hydrograph at each flow injection point (see Figure 2-3), computed through hydrological modelling as discussed in Section 2.4. The ocean boundary of the domain is forced by the local time-varying sea level corresponding to a mean high water springs tide (MHWS), phased with the peak of the flood at the largest river mouth of the domain. For each coastal domain, a point offshore from the domain was selected and a MHWS tidal cycle was extracted at this point from the NIWA tidal model[6]. Thus, appropriate values for MHWS were used for each different domain. See Table 2-1 for MHWS amplitudes used for specific domains.

The grid resolution is a critical parameter for the simulation that drives both the results numerical accuracy and the simulation time. While rapid estimates of the hydrodynamics within the floodplains can be obtained on a coarse grid, such results possess a high level of numerical errors introduced by the rough interpolation of the topography, staircasing of boundaries, and numerical discretisation errors. On a fine grid, the numerical errors are significantly reduced at the expense of increased computational time. An appropriate compromise between accuracy and computational time must be found. The solution to this is to refine the domain only around the boundaries of permanent flow paths (i.e., critically, around the stopbanks) and in general where flooding is expected while leaving the rest of the domain at a coarser resolution for the sake of computational speed. Critically, BG-Flood can operate with grids that feature local refinements at locations of interest.

To achieve this, first, a coarse resolution model with a uniform grid spacing is calculated over the entire domain, for fluvial flooding. The results from this coarse modelling are then used to develop targeted grid refinement in locations of interest using the adaptative mesh method implemented in

[6] https://tides.niwa.co.nz/

BG-Flood. Other information such as the locations of stopbanks and river and streams (both generated in Section 2.2) are also used to identify where high-resolution modelling is needed. Figure 2-10 shows an example of a refinement grid developed for the Manawatū domain. This grid is used to set the resolution of the adaptive grid used in the higher resolution modelling. The high-resolution target will be imposed, then the resolution will transition progressively to lower resolutions (or other levels imposed on the map). The map presenting a “minimum” resolution of the final model.

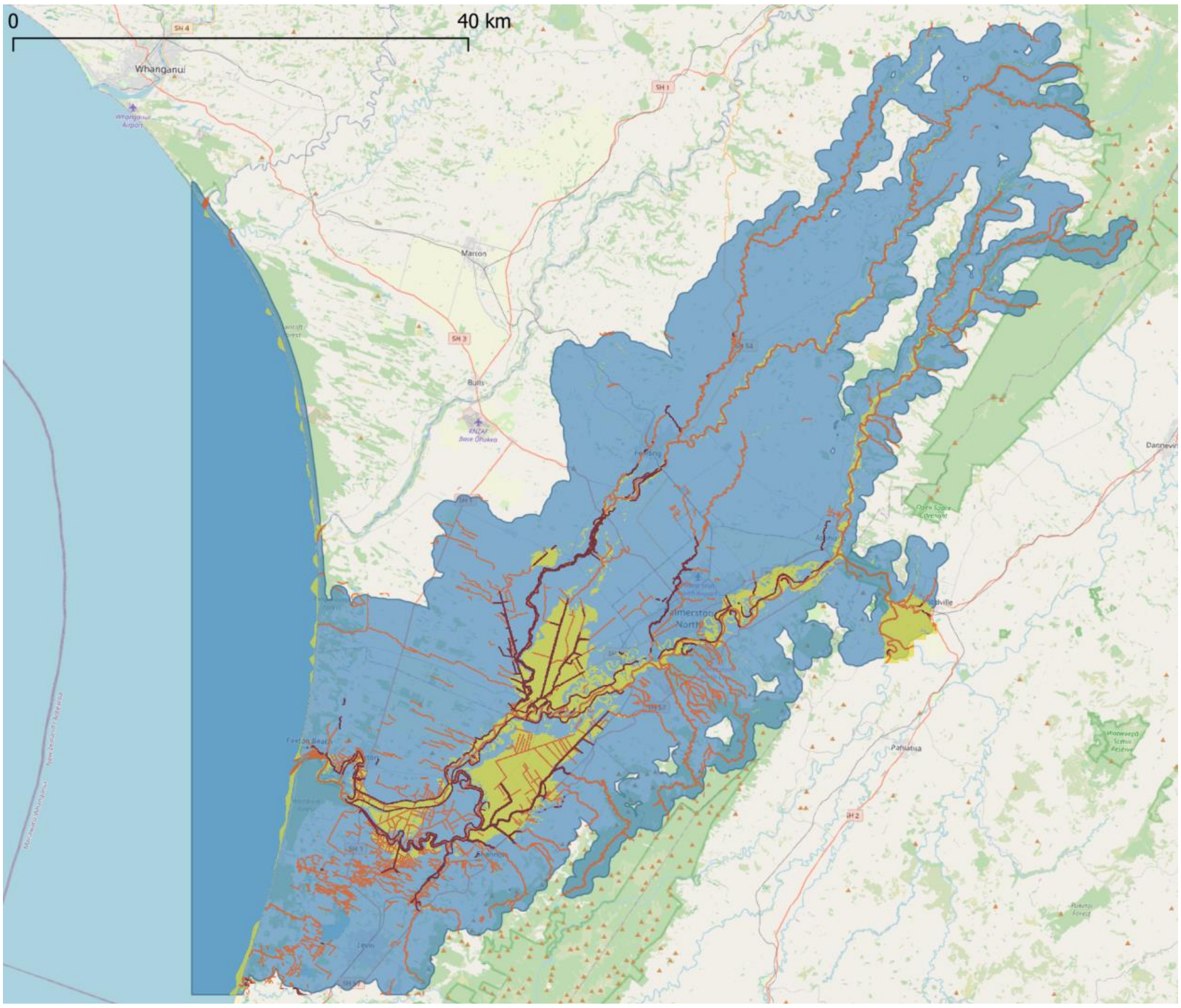


**Figure 2-10: Target refinement map generated for the Manawatū domain, 200-year ARI, current conditions.** Red, orange and yellow correspond to an 8 m resolution target due to stopbank, rivers and streams or expected flooded area respectively. Blue area: minimum resolution of 64 m.

Finally, the BG-Flood model produces time-varying maps of water elevation, velocity and water depth, as well as specific risk assessment variables such as the product of water depth and velocity. The chosen time resolution was one hour. The maximum water depth, mean water depth rising rate up to a depth 1.2 m, and the maximum value of the product of depth and velocity at each location throughout the simulation are then extracted and projected on an 8 m grid for use in the risk assessment model.

## 2.6 Climate change methodology

Climate change scenarios were modelled for the 200-year design storm inundation for +1˚C, +2˚C, +3˚C above current climate (which correspond to +2˚C, +3˚C, +4˚C above the pre-industrial climate, respectively). For coastal locations, we also modelled the 200-year +3˚C design storm scenario with sea level rise (SLR) as a sensitivity test to see how much this affected the inland flooding results.

Climate change flood inundation scenarios were not modelled for design storms with lower ARIs. Instead, we provide indicative mappings between these lower ARIs with climate change and the higher ARIs (including the 200-year climate change scenarios) in Table 2-3. These mappings were calculated using three proxies, namely (i) by comparing the change in the peak flow of the largest river within the domain at the outflow to the sea; (ii) by comparing the change in the maximum rainfall in the design storm; and (iii) by comparing the total rainfall in the design storm. The ranges given in Table 2-3 represent the spread of the three methods. For climate change scenarios that map onto ARIs larger than a 200-year event, the mapping gives the 200-year ARI plus warming equivalent.

Figure 2-Figure 2-11 shows the example for the Whanganui catchment. Based on the three proxies (peak flow, maximum rainfall and total rainfall) curves are developed for the different ARIs under warming conditions. Using the peak flow as a proxy, the 20-year event with one degree of additional warming maps on to a 134-year event; using maximum rainfall, the 20-year event maps onto a 200-year event with 0.1˚C additional warming; and using total rainfall, it maps onto a 150-year event. Thus, the range given in Table 2-3 is from a 134-year event to a 200-year event with 0.1˚C additional warming.

These climate change models based on temperature increases can be correlated to a given Shared Socio-Economic Pathway (SSP) scenario and time-period as required. For example, for the map of the 200-year event with +1˚C and for the SSP3-7.0 scenario, this scenario is projected to reach 2˚C above the pre-industrial climate around 2045 and so that is when that map would be valid as the 200-year event. Conversely, if one wanted the 200-year event for SSP5-8.5 for the end of the century, the average expected temperature increase is 3.1˚C above current climate and so the 200-year +3˚C map would be the appropriate one to use.

To evaluate the impact of sea level rise on flood maps for the climate change scenarios, a complementary 200-year, +3 ˚C above sea level was run in the stopbanks-up and stopbanks-down configuration, by adding a 1.5m of sea level on top of the MHWS for the on the Pacific side (East Coast on Table 2-1) and a 1.1m of sea level rise on top of the MHWS for the Tasman Sea catchments (West Coast on Table 2-1). These values were selected by considering the global sea level rise associated with SSP scenarios for four degrees above pre-industrial levels as well as the expected ground deformation. Because this was a sensitivity test on how the sea level rise affects freshwater flooding, we used the largest relative sea level rise (i.e., including both global sea level rise and vertical land movement) expected for each of the two Horizons coasts.

The method used to calculate the sea level rise increments used was based on global temperature increases for different SSP scenarios taken from Figure SPM.8 in (IPCC 2021). Under SSP3-7.0, three additional degrees of warming is expected to be reached around 2105 with a commensurate sea level rise of 0.92 m. Under SSP5-8.5 it is expected to be reached in 2080 with a commensurate sea level rise of 0.55 m. Vertical land movement estimates were taken from NZSearise[7]. On the East Coast of the Horizons region all coastal regions are sinking, with the fastest rate of movement being -

[7] https://www.searise.nz/

7.2 mm/year. This gives an extra 57.6 cm between now and 2105. Adding these together gives a maximum relative sea level rise of 1.5 m for three degrees of additional warming on the east coast of Horizons Region. For the west coast of the Horizons Region the coastal areas are neutral to sinking with a maximum rate of movement being -2.5 mm/year. This is equivalent to an extra 20 cm between now and 2105. So, for the west coast catchments we used a relative sea level rise of 1.1 m.

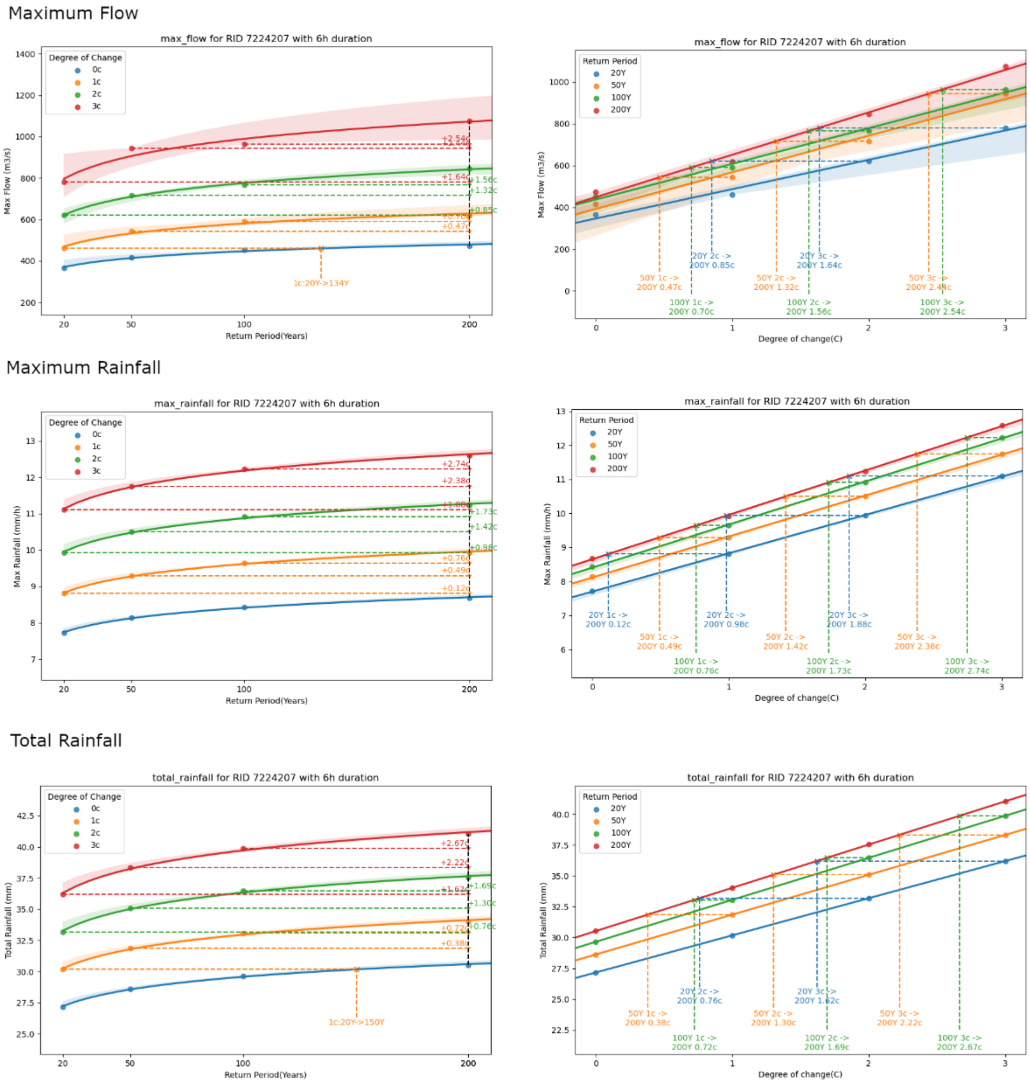


**Figure 2-11: Example mapping for lower ARI events under climate change.** These are the mapping for the Whanganui catchment. The top row uses maximum flow as the proxy; the middle row, maximum rainfall; and the bottom row, total rainfall. The left-hand column maps the lower ARIs plus warming to higher ARIs. Where the higher ARI is greater than a 200-year rainfall event the right-hand column maps to 200-year plus warming events.

**Table 2-3: Increases in apparent ARI due to climate change.** The mapping for 20-year, 50-year and 100-year rainfall events under climate change warming to equivalent higher ARIs and 200-year events plus climate change were calculated by three metrics and this table gives the range.

| Location | ARI | +1˚C | +2˚C | +3˚C |
|---|---|---|---|---|
| Ākitio | 20-year | 33-year to 39-year | 58-year to 78-year | 84-year to 161-year |
| | 50-year | 81-year to 110-year | 177-year to 200-year+0.2˚C | 200-year+0.6˚C to 200-year+1˚C |
| | 100-year | 200-year to 200-year+0.2˚C | 200-year+0.8˚C to 200-year+1.1˚C | 200-year+1.6˚C to 200-year+2˚C |
| Ōhau-Levin | 20-year | 41-year to 49-year | 83-year to 125-year | 169-year to 200-year |
| | 50-year | 114-year to 141-year | 200-year+0.3˚C to 200-year+0.6˚C | 200-year+1.1˚C to 200-year+1.5˚C |
| | 100-year | 200-year+0.2˚C to 200-year+0.4˚C | 200-year+1.1˚C to 200-year+1.3˚C | 200-year+2.1˚C to 200-year+2.3˚C |
| Whanganui | 20-year | 134-year to 200-year+0.1˚C | 200-year+0.8˚C to 200-year+1˚C | 200-year+1.6˚C to 200-year+1.9˚C |
| | 50-year | 200-year+-.4˚C to 200-year+0.5˚C | 200-year+1.3˚C to 200-year+1.4˚C | 200-year+2.2˚C to 200-year+2.4˚C |
| | 100-year | 200-year+0.7˚C to 200-year+0.8˚C | 200-year+1.6˚C to 200-year+1.7˚C | 200-year+2.5˚C to 200-year+2.7˚C |
| Upper Manawatū | 20-year | 38-year to 50-year | 78-year to 130-year | 177-year to 200-year+0.5˚C |
| | 50-year | 98-year to 145-year | 200-year+0.3˚C to 200-year+0.6˚C | 200-year+1˚C to 200-year+1.5˚C |
| | 100-year | 200-year+0.2˚C to 200-year+0.4˚C | 200-year+1˚C to 200-year+1.3˚C | 200-year+2.1˚C to 200-year+2.3˚C |
| Taumarunui | 20-year | 47-year to 58-year | 108-year to 176-year | 200-year+0.2˚C to 200-year+0.7˚C |
| | 50-year | 131-year to 168-year | 200-year+0.5˚C to 200-year+0.8˚C | 200-year+1.3˚C to 200-year+1.6˚C |
| | 100-year | 200-year+0.3˚C to 200-year+0.5˚C | 200-year+1.3˚C to 200-year+1.4˚C | 200-year+2.2˚C to 200-year+2.4˚C |
| Manawatū | 20-year | 51-year to 65-year | 130-year to 200-year+0.1˚C | 200-year+0.4˚C to 200-year+0.9˚C |
| | 50-year | 147-year to 193-year | 200-year+0.6˚C to 200-year+0.9˚C | 200-year+1.4˚C to 200-year+1.8˚C |
| | 100-year | 200-year+0.4˚C to 200-year+0.5˚C | 200-year+1.2˚C to 200-year+1.5˚C | 200-year+2.2˚C to 200-year+2.4˚C |
| Whangamōmona | 20-year | 34-year to 39-year | 57-year to 77-year | 95-year to 154-year |
| | 50-year | 90-year to 105-year | 166-year to 200-year+0.2˚C | 200-year+0.5˚C to 200-year+1˚C |
| | 100-year | 199-year to 200-year+0.2˚C | 200-year+0.9˚C to 200-year+1.1˚C | 200-year+1.7˚C to 200-year+2˚C |
| Wainui-Herbertville | 20-year | 33-year to 38-year | 55-year to 73-year | 90-year to 143-year |
| | 50-year | 91-year to 106-year | 166-year to 200-year+0.3˚C | 200-year+0.5˚C to 200-year+1˚C |

| Location | ARI | +1˚C | +2˚C | +3˚C |
|---|---|---|---|---|
| | 100-year | 200-year to 200-year+0.2˚C | 200-year+0.9˚C to 200-year+1.1˚C | 200-year+1.8˚C to 200-year+1˚C |
| Ohakune | 20-year | 36-year to 42-year | 63-year to 87-year | 110-year to 188-year |
| | 50-year | 96-year to 115-year | 187-year to 200-year+0.3˚C | 200-year+0.6˚C to 200-year+1.1˚C |
| | 100-year | 200-year to 200-year+0.2˚C | 200-year+1˚C to 200-year+1.1˚C | 200-year+1.9˚C to 200-year+2.1˚C |
| Turakina | 20-year | 36-year to 46-year | 73-year to 106-year | 139-year to 200-year+0.2˚C |
| | 50-year | 104-year to 134-year | 200-year+0.1˚C to 200-year+0.4˚C | 200-year+0.9˚C to 200-year+1.3˚C |
| | 100-year | 200-year+0.1˚C to 200-year+0.4˚C | 200-year+1˚C to 200-year+1.2˚C | 200-year+1.9˚C to 200-year+2.2˚C |
| Aohanga | 20-year | 32-year to 40-year | 60-year to 82-year | 103-year to 172-year |
| | 50-year | 96-year to 113-year | 184-year to 200-year+0.3˚C | 200-year+0.7˚C to 200-year+1.1˚C |
| | 100-year | 200-year+0.1˚C to 200-year+0.3˚C | 200-year+1˚C to 200-year+1.2˚C | 200-year+1.7˚C to 200-year+2.1˚C |
| Rangitīkei | 20-year | 41-year to 48-year | 81-year to 121-year | 163-year to 200-year+0.4˚C |
| | 50-year | 112-year to 137-year | 200-year+0.2˚C to 200-year+0.6˚C | 200-year+1˚C to 200-year+1.4˚C |
| | 100-year | 200-year+0.2˚C to 200-year+0.4˚C | 200-year+1.1˚C to 200-year+1.3˚C | 200-year+1.9˚C to 200-year+2.2˚C |

### 2.6.1 Use of HIRDS v4 (Climate Change temperature increments) with SSP/RCP scenarios

Climate change is accounted for in HIRDS v4 (Carey-Smith et al. 2018) in terms of temperature increments. Often future climate change projections are given in terms of the Shared Socio-economic Pathway (SSP) or the Representative Concentration Pathway (RCP) (IPCC 2021). The SSP or RCP is a projection of the future that accounts for increases in atmospheric $CO_2$. These pathways chart how atmospheric $CO_2$ levels are expected to change over time and using Earth Systems Models (ESM), the changes in global temperature based on the atmospheric $CO_2$ are also mapped. Variation in the different ESM models lead to variations in the temperature projections meaning that for each future time and SSP or RCP scenario there will be a range of possible temperature increases. Figure 2-12 shows the projected temperature increases based on different SSP scenarios (reproduced from IPCC 2021).

There are two ways that that the modelling can be connected to the SSP/RCP scenarios depending on whether you are starting from the modelling with a given temperature increment or whether you are starting from a future scenario.

Current climate is already around 1˚C above preindustrial. If you are starting from the modelling, and are interested in when a simulation for a given temperature increment and AEP is valid (e.g., 0.5% AEP +1˚C), the +1˚C scenario is equivalent to 2˚C above pre-industrial which could be reached between approximately 2040 to 2060 (earlier for SSP5-8.5, later for SSP3-7.0, later still for SSP2-4.5 and this level of warming may not be reached in scenarios SSP1-2.6 and SSP1-1.9). So, the 0.5% AEP +1˚C simulation represents the 0.5% AEP expected around that timeframe. Likewise, the earliest the +2˚C simulations are likely to be valid for is around 2060, but if we are on SSP2-4.5 it may not be reached until after 2100.

The other way this information can be used is for a given SSP and timeframe. Say for 2100 for SSP3-7.0, Figure 2-12 shows that the expected temperature increase is +3˚C. The shaded colour shows that the "most likely" range for the temperature increase is from +2˚C to +4˚C above current climate.

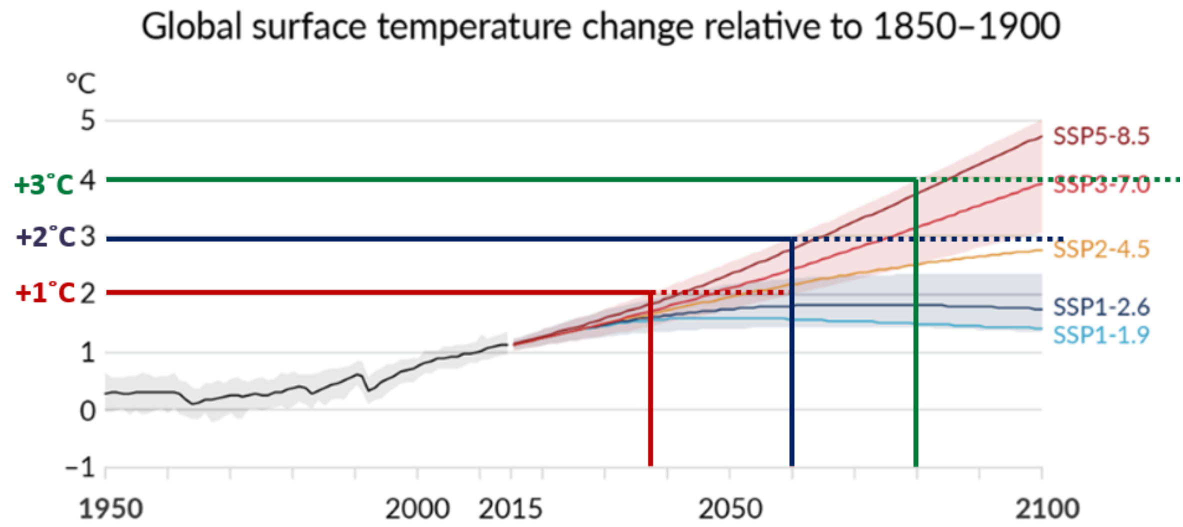


**Figure 2-12: Global surface temperature changes 1950-2100 as a difference to the 1850-1900 period for different SSP scenarios.** Shaded colours represent the "very likely" range for scenarios SSP3-7.0 (red) and SSP1-2.6 (blue/grey). The current epoch is around 1C above 1850-1900 (pre-industrial period) so the red, navy and green thick lines show when +1˚C, +2˚C, +3˚C above current climate could occur. Underlying figure is Figure SPM.8 panel (a) from the IPCC 6th Assessment Report WGI Summary for Policy Makers.

# 3 Results

The modelling was undertaken on the high-performance computing facility of NeSI (the New Zealand eScience Infrastructure), on A100 GPUs with runtime durations between 5h to 20h, depending on the domain size and physical duration of the modelled event. Several hundred to fifteen hundred rivers and streams were injected into the flood inundation domains depending on the complexity and size of the domain.

## 3.1 List of scenarios

### 3.1.1 Hydrological models

The hydrological model TopNet was used as a step in the generation of inundation maps. It was also used to determine the time of concentration of each catchment (i.e., the duration of the storm that produces the largest discharge) and to generate a mapping of a wide range of climate change scenarios to the scenarios for which the inundation maps were generated (see Section 2.6). This method is used for larger exploration of the parameters as the hydrological model and design storm generator are less computationally demanding. For the 12 domains presented in Section 2.1, we simulated the 20-, 50-, 100- and 200-year ARI design storm events for all durations from 6h to 72h with a 6h increment and for actual climate conditions, +1˚, +2˚, +3˚ Celsius above current climate conditions, which results in 2,112 models.

### 3.1.2 Inundation models

The full workflow presented in Section 1 was used to produce a set of flood maps. For the 12 domains presented in Section 2.1, we simulated a 20-, 50-, 100-, 200-year ARI design storm event for actual climate conditions. We also simulated a 200-year ARI design storm event for +1˚, +2˚, +3˚ Celsius above actual climate conditions. For all these design storms scenarios, we model the inundation with the actual stopbanks, but also a stopbanks-down configuration (see Section 2.2). Even though the effect of sea level rise is out of the scope for this study, we simulated scenarios for all the coastal domains for the 200-year ARI rain storm with +3˚ Celsius above current climate conditions, with a realistic to large sea level rise (see Section 2.6). This aims to evaluate the maximum inland influence of sea level rise for climate change scenarios. This represents 146 inundation models. See Figure 3-1 for an overview of the flood maps.

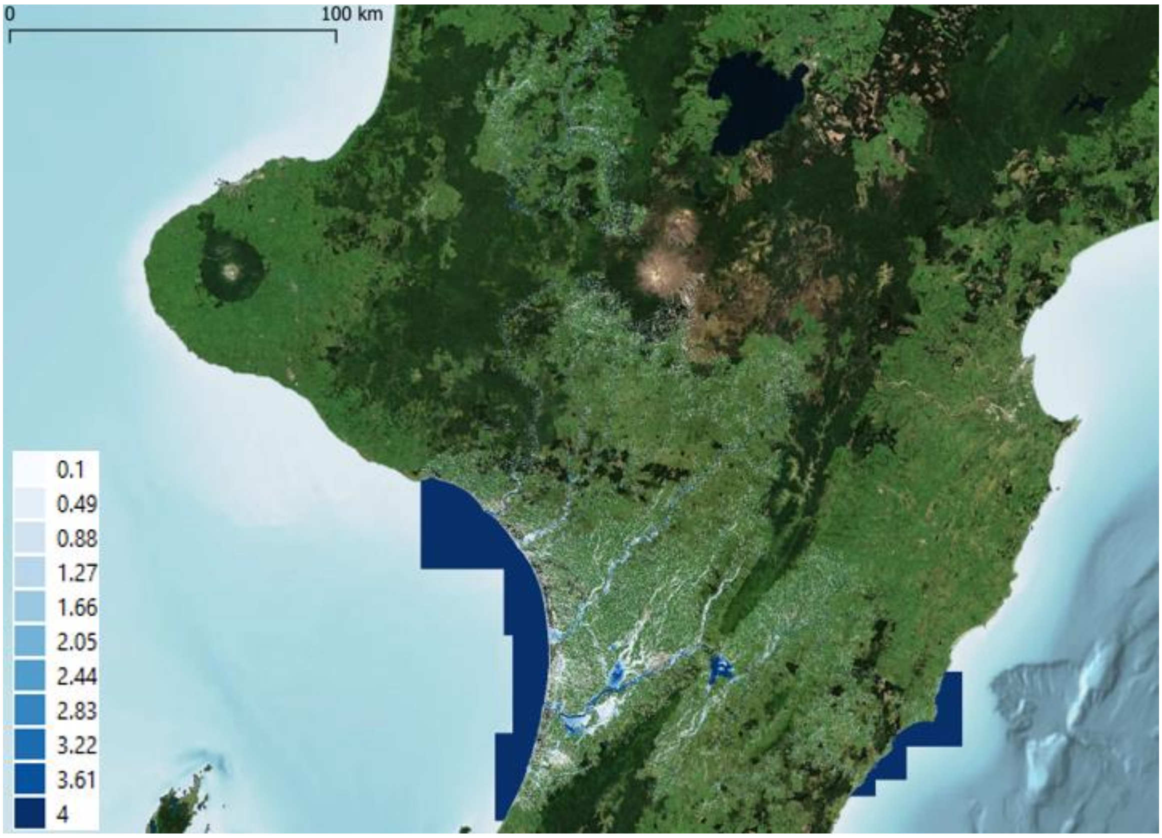


**Figure 3-1: Overview of the flood maps.** Maximum water depth for the 200-year ARI scenario, current climate conditions for all the computational domains.

For the Manawatū domain (lower Manawatū), the maximum discharge in the Manawatū Gorge was initially around 3400 $m^3s^{-1}$, lower than what was observed in the Upper Manawatū domain, where 3900 $m^3s^{-1}$ was observed. During the generation of the design storm for each domain, a reduction factor is applied, function of the area of the catchment. For the Manawatū domain, the full area of the Manawatū catchment is used, producing a larger reduction factor than for the Upper_Manawatū domian, where only the area above the gorge is considered. Which then explain a lower storm intensity in the Manawatū domain and lower discharge through the Manawatū gorge in this domain. The Manawatū domain model has been modified to increase the river injections above the Manawatū Gorge to reach a similar discharge of 3900 $m^3s^{-1}$ as observed in the Upper Manawatū model and similar to the value calculated in the flood statistical analysis associated to this study (see Singh, 2025).

## 3.2 Water depth maps

During the simulation, different 2D variables are saved in a NetCDF file at regular time steps of one hour. Some variables such as the water elevation above NZVD2016 (m); the water depth (m); the velocity vector (m $s^{-1}$) are exported as snapshots at these output times; other variables are computed as the maximum values between the beginning of the simulation and the current output step. To the latter category belong the maximum of water elevation above NZVD2016 (m); the maximum of water depth(m); and the maximum of water depth times velocity($m^2s^{-1}$). For conciseness and as needed for the risk assessment, maximum values at the end of the simulations have been extracted, especially for maximum water depth, maximum water depth times velocity and maximum water elevation. Using the time evolution of the water depth every hour, we also extracted the rising rate for each grid cell for the first 1.2 m of inundation. The different flood maps generated are listed in Appendix A.

Figure 3-2 shows sample results of the flood extents for difference scenarios for the lower Rangitīkei domain and Figure 3-3 shows a zoom-in around the Ohakea-Bulls area.

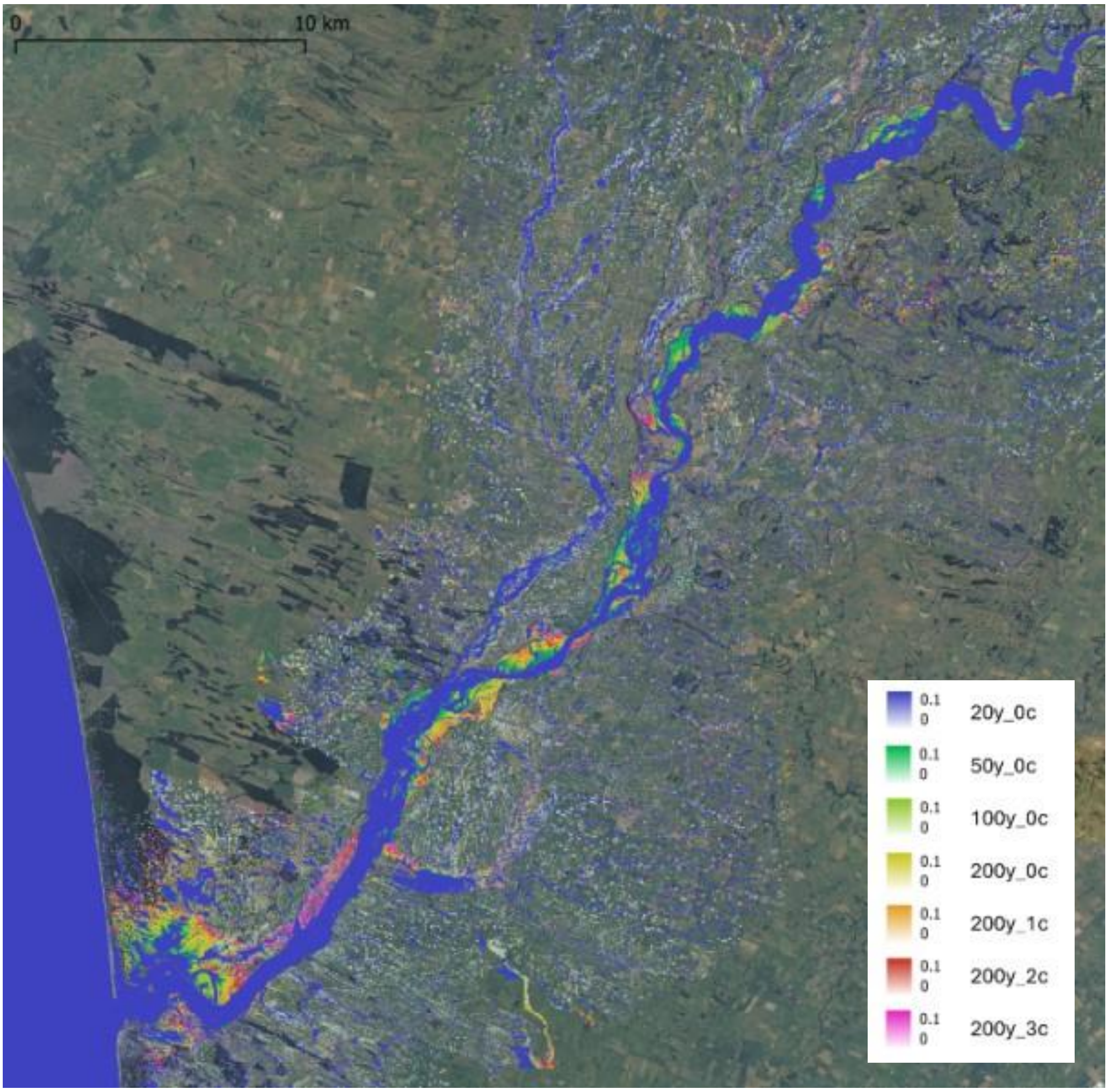


**Figure 3-2: Flood extent for the design storm scenario for the lower Rangitīkei domain.** Areas are considered as flooded if the local value of the maximum water depth exceeds 0.1 m. Each colour represents a scenario from 20-year ARI for current climate conditions in blue, through 200-year ARI for current climate conditions in yellow to 200-year ARI +3˚C climate change conditions in purple. The figure refers to the stopbanks-up configuration.

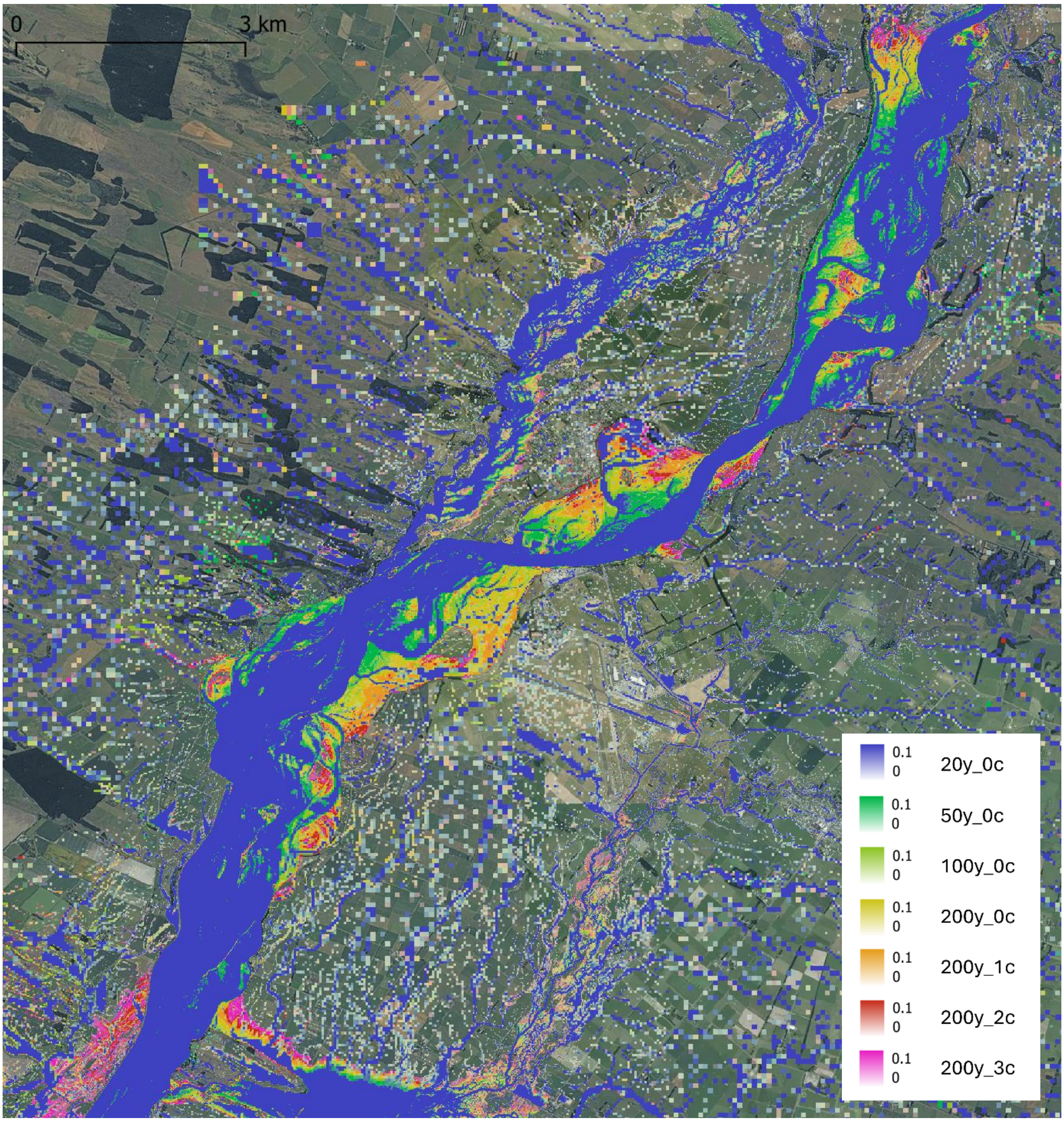


**Figure 3-3: Flood extent for the design storm scenarios for the lower Rangitīkei domain, zoomed into the Ohakea-Bulls area.** Areas are considered as flooded if the local value of the maximum water depth exceeds 0.1 m. Each colour represents a scenario from 20-year ARI for current climate conditions in blue, through 200-year ARI for current climate conditions in yellow to 200-year ARI +3˚C climate change conditions in purple. The figure refers to the stopbanks-up configuration.

## 3.3 Contrasting the stopbanks-up and stopbank-down scenarios

As explained in Section 3.1.1, for each design storm scenario, we modelled the flood with and without stopbanks. The method used to remove the stopbanks is to use the stopbanks database and remove all the elevation along these lines (see Section 2.2 for more details). We are then removing all the stopbanks at the same time. This can inform on residual risk but may likely underestimate flooding resulting from a stopbank breach. Figure 3-4 is an example of the results obtained for the Rangitīkei catchment, for different ARI and climate change scenarios.

**Figure 3-4: Flood extent with stopbank and without stopbanks for the lower Rangitīkei area.** Left: 20-year ARI in current climate conditions with (blue) and without stopbanks (white). Centre: adding to the left map a 200-year ARI in current climate conditions with (yellow) and without stopbanks (white). Right: adding to the centre map a 200-year ARI + 3˚C of climate change warming with (purple) and without (white) stopbanks.

## 3.4 Sea level rise (SLR) influence

In order to evaluate the influence of sea level rise on the results, we also considered sea level rise for the most extreme scenario explored (see Section 2.6). For all the domains, the influence of the sea level rise is concentrated in the coastal area. For the East Coast catchments, with a 1.5 m increase of SLR, most of the effect was confined to a 250 m-wide band along the coastline, and to small streams up to 2 km inland (see Figure 3-5). For the West Coast catchments, a 1.1 m increase of sea level rise resulted in a slightly larger extent of the flood on the coast and in main river mouths. We observed an increased flooding by back water effect in the Manawatū River mouth up to 5 km inland (see Figure 3-6) and up to 10 km inland on the Whanganui River. Finally, the influence of sea level rise on these 200-year ARI design rainstorm flood is very limited in the coastal area (in the first hundreds to thousands of metres from the shoreline) and the flooding is largely resulting from fresh water, fluvial and pluvial flooding.

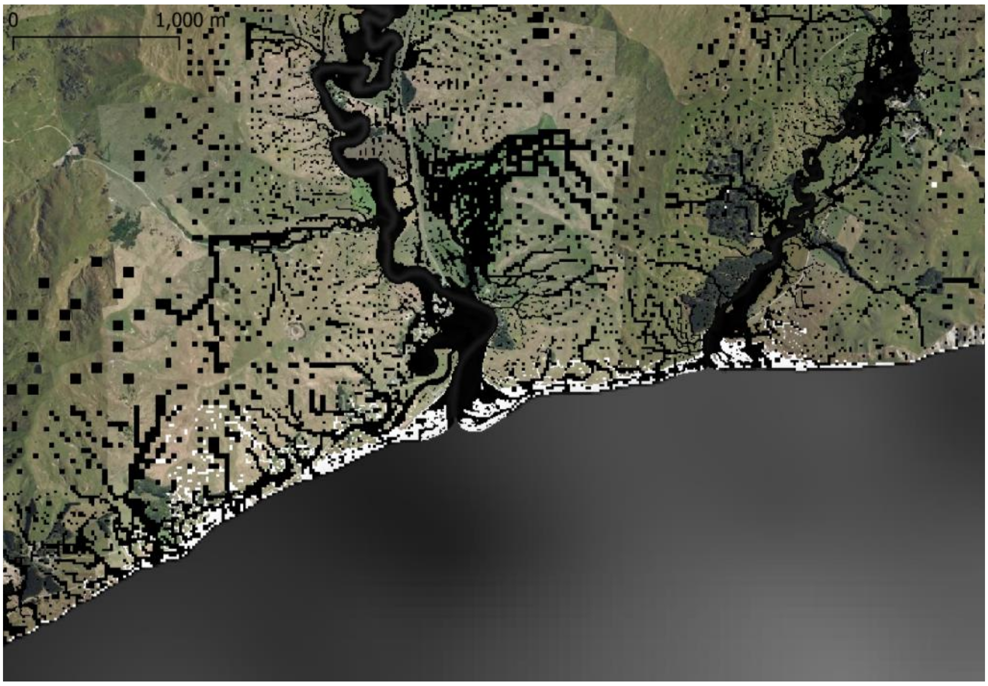

Figure 3-5: Inundation extend with (white) and without (black) sea level rise for the 200-year +3˚C scenario. Herbertville, Wainui-Herbertville domain.

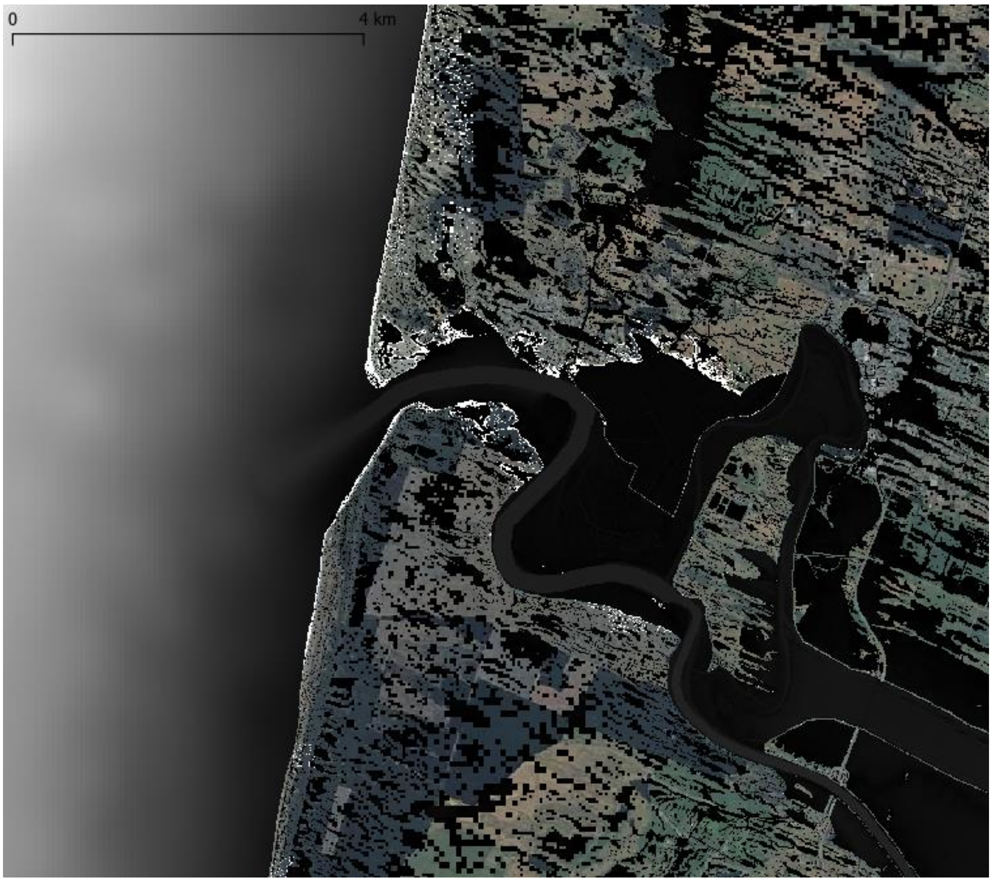


**Figure 3-6: Inundation extend with (white) and without (black) sea level rise for the 200-year +3˚C scenario. Manawatū river mouth.**

## 3.5 Limitations

### 3.5.1 LiDAR data coverage

The availability of LiDAR data is often the first limitation in the type of modelling of this report, especially due to the requirements of a full 2D approach (compared with a 1D or combined 1D-2D methods). The modelling approach used here was developed for the national flood assessment project and initially limited to areas where recent LiDAR was accessible. To increase the coverage, some DEM and DSM data were also used for this regional mapping, creating issues with the vertical projection.

Furthermore, unlike DEMs, DSMs do not represent the ground elevation but the surface elevation. For instance, this implies that DSMs represent treetop elevation instead of ground elevation in areas covered by vegetation. This can create unrealistic obstacles to flow paths. The hydrological conditioning of the DEM and the opening of streams and rivers can remove some obstacles to river flows like overhanging trees, but some unrealistic flow constrictions can persist. As no correction is applied to land DSM, overland flow paths can be affected.

The limitation of the LiDAR coverage and use of complementary input information also impact the definition of the roughness layer. The roughness length, related to the roughness of the ground or ground cover which affects the speed of water flow, can be related to the above-ground LiDAR point cloud. Other methods relying on national or regional database of land-cover have been tested but do not give the granularity of roughness changes that can be achieved with LiDAR. LiDAR data is then key to the methodology. Therefore, in this work we have chosen the simple approach of assigning a default roughness length where no LiDAR data was available.

### 3.5.2 Stopbank information

Stopbank information is critical for inundation modelling of area around flood protection infrastructures. Precise locations (and extents) are important to enforce the locations and crest heights of these structures, especially around small streams where the approximate stopbanks position might overlap the stream and cut it off. For larger rivers, the position is less critical, but elevation information can better inform the stopbank enforcement in the model. Lastly, for thin structures such as flood walls, the elevation information is crucial as they can be difficult to detect on LiDAR.

### 3.5.3 Resolution issues

For this project, an 8m resolution DEM is used. Consequently, any stream with a cross-section narrower than 8 or even 10 m has not been well represented. In the region, we particularly observed for small streams surrounded by flood protections, enforcing the flood protection in the DEM often resulted in blocking the stream flow due to the narrowness of the gap between stopbanks being a similar size to the resolution of the DEM. In these situations, a very small misalignment of the stopbank can also have a similar result and cut off the stream flow.

### 3.5.4 Flood map refinement and pixelisation

As explain in the methodology, the computational meshes presents different levels of resolution, with high resolution in river and streams, stopbanks and where fluvial flooding is expected from a coarse model. This might result in large pixels in places where there wasn't flooding in the coarse resolution model (such as small tributaries) or pluvial flooding if the pixels are discontinuous.

There are methods that can be used to interpolate coarse flooding down to a finer resolution, but these methods can be misleading because the results visually suggest an accuracy that may not be warranted. We would rather show the results at the resolution of the modelling because that way the user can see the inherent uncertainty in the results. If some of these specific places show a high risk (a combination of high hazard and assets of interest), the model refinement map can be modified to ensure high resolution in this area of interest, and the final high-resolution modelling redone.

Similarly, rain-on-grid modelling can generate isolated pixels of flooding that could be "cleaned" by methods based on water depth threshold and flooded area. However, they can be misleading too, as results are sensitive to the parameters chosen and should be adapted to the specific use of the flood maps. Again, for this report, the raw modelling results have been presented rather than post processing them.

### 3.5.5 River and river mouth bathymetry

Finally, the river bathymetry cannot be extracted from the type of LiDAR (red LiDAR) available for the region. Manual 'digging' of the lower part of the river informed by cross-section data has been applied so as to ensure that the river bathymetry is represented at least approximately. The use of the cross-sections to generate a realistic river bathymetry was out of the scope of this work. Some river mouths have been dug out using the method implemented in GeoFabrics, which can be further improved if cross sections are available in the river mouth area.

### 3.5.6 A semi-automatic workflow

Finally, these maps have been generated by a semi-automatic workflow. Even if some tests and modifications have been implemented for this project, any manual fix to the models or DEMs was out of the scope of this project. Some avenues to improve these models would be to manually realign some stopbanks or push them further from small streams for example. The intersection between stopbanks and streams can also be refined by considering these as gates open or closed during a flood event. Finally, culverts were extracted from OpenStreetMaps database, and some might be missing in the region.

## 3.6 Use of this data and recommendations

This regional modelling is not validated or calibrated to the same level that a local- or catchment-scale model would be. While some of the criteria are level B/C, other criteria are only at level A giving it an overall level of A. Not all flood structures are fully represented and there may be some artifacts in the DEM and roughness maps. The resolution of 8 m means that smaller river channels may not be fully resolved. These flood model outputs do, however, give a good indication of the scope of the flood hazard and risk that Horizons faces and how this is likely to change under climate change. Their use is appropriate to understand aggregated risk in terms of the order of magnitude of the problem. Additionally, these flood outputs can be used as a screening tool to identify where the highest levels of risk are likely to be and where further work (further LiDAR acquisition, higher level modelling etc.) is warranted to better characterise the flood hazard, risk and vulnerability.

The main recommendations from this report for future work are:

- **Pluvial vs Fluvial flooding**: run fluvial only model around identified towns/areas of interest to differentiate between the two flooding mechanisms
- **Improvements to inputs**: work with Horizons to identify best places to improve input data (e.g., LiDAR coverage, stopbank locations and elevations). Models could be rerun incorporating this improved information and potentially at a higher resolution (e.g., 4 m)
- **Residual Risk**: Identify locations where stopbanks are overtopped in scenarios. From these select stopbank breach scenarios of interest to model assuming that overtopping could cause failure of stopbanks
- **Extra-tropical Cyclone Scenarios**: Develop an extra-tropical cyclone scenario and model this to understand the possible impacts of a direct impact on Horizons Region by an extra-tropical cyclone.
- **Bridge Heights**: Compare flood maximum elevation levels to bridge heights to estimate at what AEP individual bridges could become too dangerous for people to use.
- **Differences in Regional Model**: Case studies to understand differences between regional modelling and higher-level local modelling.

# 4 Conclusion

NIWA and WSP New Zealand Ltd are collaborating to inform the Horizons Regional Council's flood vulnerability assessment. As part of this project, NIWA provided a region-wide flood hazard assessment to contribute to the regional flood risk assessment. A set of inundation flood maps were developed using a cascade of tools, following a semi-automated procedure named 'workflow'. Workflow comprises identification of the flood modelling domain, creation of the DEM, identification of design storms, hydrological and hydrodynamic modelling, and climate change analysis.

Twelve domains were identified and for each of these we generated a hydrologically conditioned DEM and a roughness map using available LiDAR data, local DEMs, DSM, ocean contours, OpenStreetMap data and other national or global databases. For each of the 12 domains identified, design storms were created with 5%, 2%, 1% and 0.5% annual exceedance probability (AEP) or 20-, 50-, 100-, 200-year ARIs for current climate conditions, and 0.5% AEP or 200-year ARI rainfall design storms climate change scenarios corresponding to +1˚C , +2˚C , +3˚C global mean temperature increase above actual conditions (or +2˚C, +3˚C and +4˚C above pre-industrial temperatures). In the upper part of the catchment, where the slopes are excessive for hydrodynamic flood modelling, we applied the TopNet hydrological model to calculate the flow discharge to be applied at the injection point of the rivers in the floodplains. In the hydrodynamic modelling domains located in the floodplains we performed a flood modelling exercise using the 2D hydrodynamic software, BG_Flood.

After a first coarse mapping of the flood, a mesh was generated, with local refinements down to 8 m resolution in areas expected to be flooded and around strategic locations such as flood defence structures or streams. The flood models were forced by hydrographs at the river injection points calculated by the hydrological model, the rain on the floodplain and an MHWS (mean high water spring) tide at the coast. The tide was phased with the peak of the flood. For the domains containing flood defence structures, a set of simulation with these structures removed (named stopbanks-down simulations) was produced. Finally, as the climate change scenarios explored did not include sea level rise, coastal domains have been tested with sea level rise for the 200-year ARI rainfall design storm with +3˚C of climate change. The influence of sea level rise was very limited in the coastal zone, most of the flooding during these storm events originated from fresh water.

Some limitations have been observed, related to the use of complementary data where no LiDAR was available, the model resolution compared to stream section especially when surrounded by stopbanks, gate modelling and some feature misalignment or missing (most can be fixed manually but this work was out of the scope of the study). For all the scenarios presented previously, 146 models were created to generate a set of flood maps. The maximum water depth along the flood, the maximum water elevation and the maximum water depth times velocity have been extracted along with the water rising rate to inform the regional flood risk assessment.

# 5 Acknowledgements

This study builds upon the workflow and tools developed for the MBIE-funded Endeavour Programme Mā te Haumaru ō ngā puna wai ō Rākaihautū ka ora mō ake tonu. We would like to thank the programme team for their contributions. Special thanks to Yinjing Lin for mapping the climate scenarios based on hydrological results. This project was also developed in collaboration with the WSP team, whose support was central, particularly in reprojecting the Manawatū DEM. We gratefully acknowledge the Horizons Regional Council for their insightful discussions and the provision of essential data, which were critical for the creation of these maps. We also thank Trevor Carey-Smith for his contributions to the design storm generation and Céline Cattoën-Gilbert for her work on the hydrological model. Finally, the author(s) acknowledge the use of the New Zealand eScience Infrastructure (NeSI) high-performance computing facilities for this research. These national facilities are provided by NeSI and funded jointly by NeSI's collaborator institutions and the Ministry of Business, Innovation & Employment's Research Infrastructure programme.

# 6 Glossary of abbreviations and terms

| | |
|---|---|
| AEP | Annual Exceedance Probability |
| ARI | Annual Return Interval (also known as Return Period) |
| DDF | Depth-Duration-Frequency |
| DEM | Digital Elevation Model |
| DSM | Digital Surface Model |
| GIS | Geographical Information System |
| GPU | Graphical Processing Unit |
| HIRDS | High Intensity Rainfall Design System |
| IDF | Intensity-Duration-Frequency |
| IPCC | Intergovernmental Panel on Climate Change |
| LiDAR | Light Detection And Ranging |
| LINZ | Land Information New Zealand |
| MHWS | Mean High Water Spring |
| NeSI | National e-Science Infrastructure |
| netCDF | Type of data file |
| NZIS | New Zealand Inventory of Stopbanks |
| NZRA | New Zealand ReAnalysis |
| NZTM | New Zealand Transverse Mercator |
| NZVD2016 | New Zealand Vertical Datum 2016 |
| OSM | Open Street Maps |
| REC | River Environment Classification |
| RPC | Representative Concentration Pathway |
| SLR | Sea Level Rise |
| SSP | Shared Socio-Economic Pathway |
| VCSN | Virtual Climate Station Network |

# 7 References


Ashcroft, K., Barnhill, D., Hodgson, E. (2025) Horizons Flood Vulnerability Assessment. Current State Analysis. WSP Client Report prepared for Horizons Regional Council

Bosserelle, C., Lane, E.M., Harang, A. (2021) BG-Flood: A GPU adaptive, open-source, general inundation hazard model. *Australasian Coasts and Ports*, Christchurch.

Carey-Smith, T., Henderson, R., Singh, S. (2018) High intensity rainfall design system: Version 4. *NIWA Client Report*, 2018022CH: 73.

Clark, M.R., Martinez, G., McMillan, H.K., Jackson, B., Gupta, H.V., Goodrich, D.C., Srinivasan, M.S., Schmidt, J., Woods, R.A. (2008) A national hydrological model for New Zealand. *AGU Fall Meeting*, San Francisco, December 2008.

IPCC (2021) Climate Change 2021: The Physical Science Basis. Contribution of Working Group I to the Sixth Assessment Report of the Intergovernmental Panel on Climate Change: 3-32. 10.1017/9781009157896.001

McMillan, H.K., Booker, D.J., Cattoën, C. (2016) Validation of a national hydrological model. *Journal of Hydrology*, 541, Part B: 800-815. http://dx.doi.org/10.1016/j.jhydrol.2016.07.043

Oliver, H.J., Shin, M., Sanders, O. (2018) Cylc: A Workflow Engine for Cycling Systems. *Journal of Open Source Software*, 3(27). 10.21105/joss.00737

Pearson, R.A., Smart, G., Wilkins, M., Lane, E., Harang, A., Bosserelle, C., Cattoën, C., Measures, R. (2023) GeoFabrics 1.0.0: an open-source Python package for automatic hydrological conditioning of digital elevation models for flood modelling. *Environmental Modelling & Software*, 170: article no. 105842. https://doi.org/10.1016/j.envsoft.2023.105842

Pirooz, A., Moore, S., Carey-Smith, T., Turner, R., Su, C.-H. (2023) The New Zealand Reanalysis (NZRA): development and preliminary evaluation. *Weather & Climate*, 42(1): 58-74. https://www.metsoc.org.nz/resources/Documents/weather_and_climate/Vol_42_pdfs/Vol_42_Pirooz_et_al.pdf

Singh, S. (2025) Appendices to Flood Frequency in Horizons Region Report of March 2025. *NIWA Client Report*, 2025162CH.

Smart, G., Aberle, J., Duncan, M., Walsh, J. (2004) Measurement and analysis of alluvial bed roughness. *Journal of Hydraulic Research*, 42(3): 227-237. 10.1080/00221686.2004.9728388

# Appendix A List of files provided

The delivered set of inundation maps consists of 2D maps, saved in .tiff format, on an 8 m x 8 m resolution grid, in a NZTM2000/NZVD2016 datum. The stopbank down configuration only applied to domains containing stopbanks, and the sea level rise (SLR) configuration only applied to coastal domains (summarised in Table A-1: List of scenarios explored for each domain.. The stopbank up and stopbank down scenarios were applied to 7 different design storm intensities corresponding to: 20-, 50-, 100-, 200-year return period in actual conditions and 200-year return period for +1˚, +2˚, +3˚C above actual conditions. Only the 200-year return period +3˚C above actual conditions was applied to the sea level rise configurations.

**Table A-1: List of scenarios explored for each domain.**

| | **Stopbank up** *20,50,100,200-year +0˚C* *200-year +1˚,2˚,3˚C* | **Stopbank up + SLR** *200-year +3˚C* | **Stopbank down** *20,50,100,200-year +0˚C* *200-year +1˚,2˚,3˚C* | **Stopbank down + SLR** *200-year +3˚C* |
|---|---|---|---|---|
| Ākitio | ✓ | ✓ | X | X |
| Manawatū | ✓ | ✓ | ✓ | ✓ |
| Aohanga | ✓ | ✓ | X | X |
| Ohakune | ✓ | X | X | X |
| Ōhau-Levin | ✓ | ✓ | ✓ | ✓ |
| Rangitīkei | ✓ | ✓ | ✓ | ✓ |
| Taumarunui | ✓ | X | ✓ | X |
| Turakina | ✓ | ✓ | ✓ | ✓ |
| Upper Manawatū | ✓ | X | ✓ | X |
| Wainui-Herbertville | ✓ | ✓ | X | X |
| Whangamōmona | ✓ | X | X | X |
| Whanganui | ✓ | ✓ | ✓ | ✓ |

For each of these scenarios, different fields extracted from computational results were:

- Maximum_Water_Depth (m) calculated at each time step in the simulation (and not from hourly snapshots outputs), reprojected on an 8 m x 8 m grid.
- Maximum_Elevation (m): maximum of water surface elevation, calculated at each time step in the simulation (and not from hourly snapshots outputs), reprojected on an 8 m x 8 m grid.
- Maximum_Depth_times_Velocity ($m^2s^{-1}$): maximum of water depth times water velocity (amplitude) calculated at each time step in the simulation (and not from hourly snapshot outputs), reprojected on an 8 m x 8 m grid. This is a specific variable output for risk assessment.

- Rising_Rate_to_1.2m ($mh^{-1}$): water rising rate up to 1.2 m, calculated from the 1-hour snapshot outputs (water depth field h(m)), reprojected on an 8 m x 8 m grid. This is a specific variable output used to assess risk to people.

All filenames follow a similar structure, for example:

"Akitio_20y_0c_Inundation_Floodmap_Maximum_Elevation.tif", which begins with the domain name "Akitio", then the design storm characteristics "20y_0c" for 20-year return period and 0˚C of climate change above actual conditions, and then the field "Maximum_Elevation" for maximum of water surface elevation.

For the results where sea level rise was added to the tide forcing, "SLR" is added at the end of the file name and "StopbanksDown" for the configurations were stopbanks have been removed from the DEM (the default configuration being the DEM including the stopbanks).

As some flood plains can be connected during large flood events by rivers or stream flowing to adjacent basins, some computational domains overlap. To clarify the results, the maximum for all domain is shown on the output maps.

By default, "Nan" (not a number) values are allocated to area in the domain where there is no water or that are outside of the computational domain. For the Maximum_Water_Depth and the Maximum_Depth_times_Velocity, a "filled" version of the output is provided, with "0" in the computational domain where there is not water (i.e. it is not flooded) but is in the computational domain.

The input files used to model these scenarios will also be provided to Horizons separately to this report.

# Appendix B Extension: 0.2% and 0.1% AEP modelling

As a variation on the contract, design storm of 0.2% and 0.1% AEP (or 500- and 1000-years return periods) have been added to the list of scenarios, for actual and climate change scenarios corresponding to +1˚C, +2˚C and +3˚C over the current climate. For these scenarios, only the stopbank up configuration has been modelled so far. The method the generate these flood maps is the same as the method described in this report. Note that the design storms based on HIRDv4 were initially only designed for return periods up to 250-years (mainly limited by the quantity of observations available in New Zealand). These results from HIRDS have been extrapolated in this study for the creation of 500-year and 1000-year events, increasing the uncertainty around their intensity.

Table B-1 presents the all the scenarios for which flood maps were generated in this study.

**Table B-1: List of scenarios explored for each domain, including the variation.**

| | Stopbank up<br>*20,50,100,200-year +0˚C*<br>*200-year +1˚,2˚,3˚C* | Stopbank up + SLR<br>*200-year +3˚C* | Stopbank down<br>*20,50,100,200-year +0˚C*<br>*200-year +1˚,2˚,3˚C* | Stopbank down + SLR<br>*200-year +3˚C* | Stopbank up<br>*500-year +0˚,1˚,2˚,3˚C* | Stopbank up<br>*1000-year +0˚,1˚,2˚,3˚C* |
|---|---|---|---|---|---|---|
| Ākitio | ✓ | ✓ | X | X | ✓ | ✓ |
| Manawatū | ✓ | ✓ | ✓ | ✓ | ✓ | ✓ |
| Aohanga | ✓ | ✓ | X | X | ✓ | ✓ |
| Ohakune | ✓ | X | X | X | ✓ | ✓ |
| Ōhau-Levin | ✓ | ✓ | ✓ | ✓ | ✓ | ✓ |
| Rangitīkei | ✓ | ✓ | ✓ | ✓ | ✓ | ✓ |
| Taumarunui | ✓ | X | ✓ | X | ✓ | ✓ |
| Turakina | ✓ | ✓ | ✓ | ✓ | ✓ | ✓ |
| Upper Manawatū | ✓ | X | ✓ | X | ✓ | ✓ |
| Wainui-Herbertville | ✓ | ✓ | X | X | ✓ | ✓ |
| Whangamōmona | ✓ | X | X | X | ✓ | ✓ |
| Whanganui | ✓ | ✓ | ✓ | ✓ | ✓ | ✓ |

The outputs for the additional modelling are provided in a similar format to the other maps.

horizons

REGIONAL COUNCIL

horizons.govt.nz

**24 hour freephone** 0508 800 800
**fax** 06 952 2929 | **email** help@horizons.govt.nz
Private Bag 11025, Manawatu Mail Centre, Palmerston North 4442